Int. Journal of Water Management and Diplomacy
e-ISSN:2717-8277 Research Article

# WATER CONFLICTS AND THE SPATIOTEMPORAL CHANGES IN LAND USE, IRRIGATION, AND DROUGHT IN NORTHEAST SYRIA WITH FUTURE ESTIMATIONS

**Fulya Aydin-Kandemir[1], Dursun Yıldız[2]**

*[1] Ege University Solar Energy Institute 35100 Bornova/İzmir, Turkey*

*[1]Hydropolitics Association, 06680 Kavaklidere/Ankara, Turkey*

*ORCID NO: 0000-0001-5101-6406*

*E-mail: fulya.aydin.kandemir@hpacenter.org*

*[2] Izmir Institute of Technology, 35430, Izmir, Turkey*

*[2]Hydropolitics Association, 06680 Kavaklidere/Ankara, Turkey*

*E-mail: dursunyildiz@hpacenter.org*

*ORCID NO: 0000-0001-5110-9960*

Corresponding author: fulya.aydin.kandemir@hpacenter.org

**Abstract**

Climate change cause instability for conflict zones in the coming years with potential socio-economic consequences in addition to environmental impacts. Decreasing water resources and rural land usage force people to migrate from rural to urban areas due to low productivity in agriculture and animal husbandry, rising food prices, and decreasing wealth levels. This study evaluates climate change impacts on northeast Syria, relatively a wetter climate zone of Syria. Within the scope of the study, it was determined to what extent land use changes and agricultural patterns throughout the region affect water use (mainly groundwater) in addition to addressing the effects of climate change on the scale of drought. Just like in this study, revealing the possible relations between the previous regional conflicts and the changes in land use, drought, and water use will be beneficial in terms of evaluating the possible threats in the future. Obviously, the changes in land use, the increase in irrigated agricultural areas, and the intensive groundwater use make the experienced situation worse. Additionally, it will be undeniable that the effects of climate change are one of the most pressing political and economic challenges in the region since the drought has also exacerbated these problems. Therefore, it is worthwhile to evaluate the potential future threat of the spread of conflicts experienced before. In entire Syria and the northeast region, it is required more attention to adapt climate change effects on water resources to peace and security.

**Keywords:** Syria, Northeast Syria, drought, irrigation, climate change, water security, hydropolitics, Geographic Information Systems

Issue: 4 2022
Int. Journal of Water Management and Diplomacy
e-ISSN:2717-8277 Research Article

## 1. Introduction

Water is vital for all living creatures. In some cultures, certain waters are believed to be holy or to possess healing qualities. However, since water is very imperatival, water scarcity can influence many relations between different communities in the world, especially in the Middle East. According to Amery (2020), no region has witnessed more water-based conflicts than the Middle East since more than 5000 years ago (earliest civilization in Mesopotamia).

The countries of the Middle East are considered with significant spatio-temporal variations in precipitation and with local surface and groundwater resources. As a Middle East country, Syria turns into increasingly scarce water as the future requirement approaches or exceeds current resources (Varela-Ortega and Sagardoy 2002; Salman and Mualla 2004).

Syria (Fig 1) includes very arid, arid, semi-arid, humid, and semi-humid climatic zones (Fig 2 and Fig 3). Different climate types arise from geographical differences in the country because of the coastal areas in the Mediterranean, deserts in the middle, and forests in the north and the northwestern regions (Albrecht, Schmidt, Mißler-Behr and Spyra, 2014). Therefore, Syria is vulnerable to climate change because of current and future climatic conditions for the Mediterranean, the Middle East, and African countries. According to Mathbout et al. (2018), the 2007–2010 drought was the driest period in the instrumental record, happening just before the onset of the recent conflict in Syria.

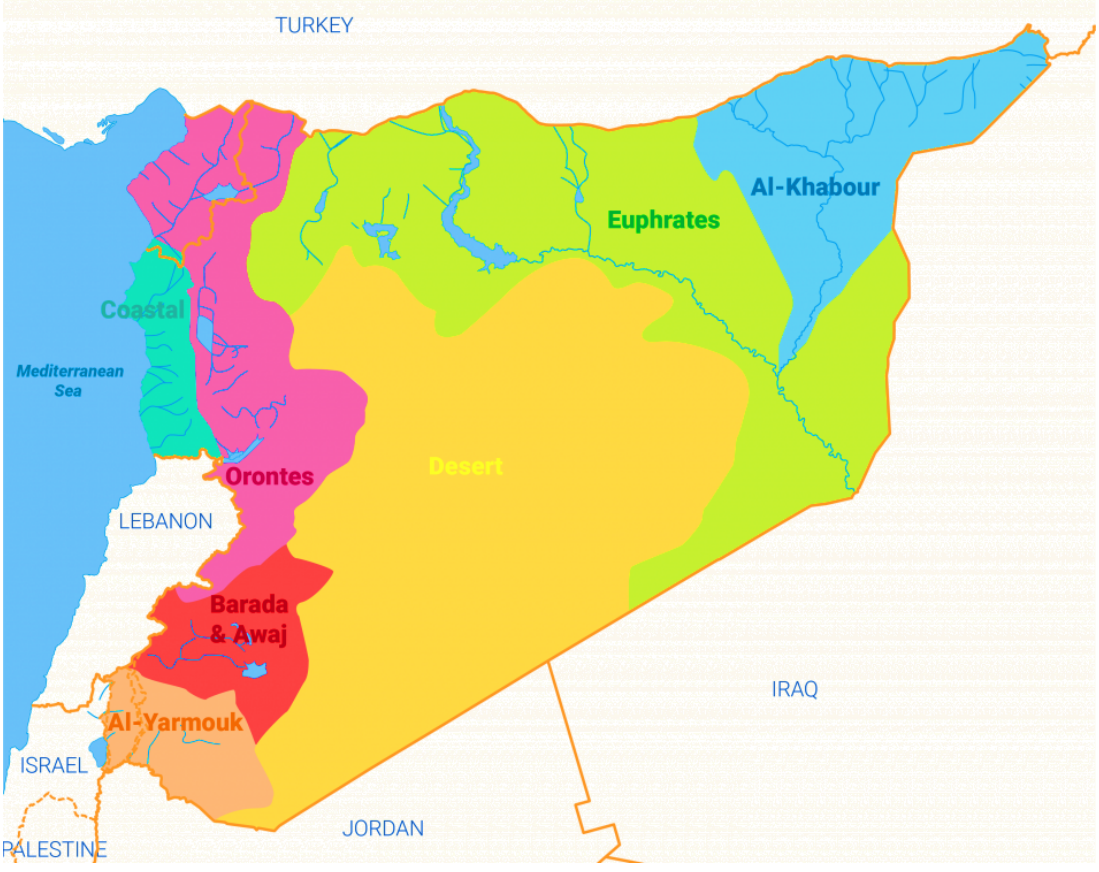


**Fig 1.** Water basins of Syria (Fanack.com, 2019).

Issue: 4 2022
Int. Journal of Water Management and Diplomacy
e-ISSN:2717-8277 Research Article

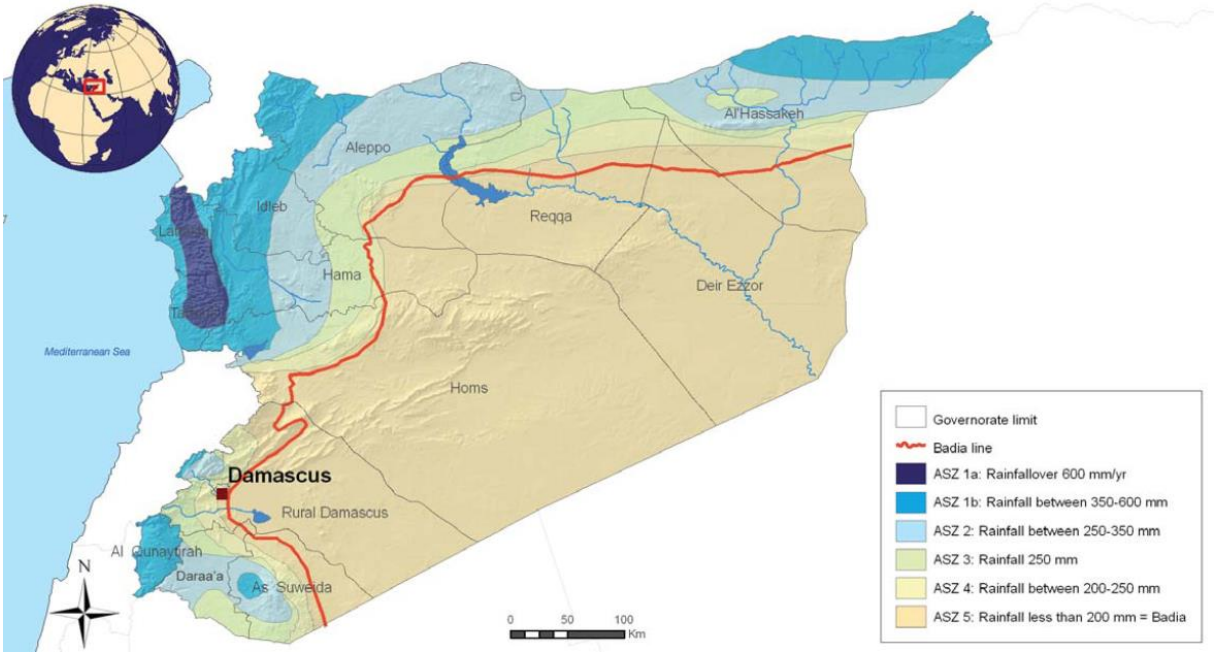


**Fig. 2.** Based on IFAD, climatic zones in Syria (IFAD, 2010).

In Fig 2, the ASZ regions are defined as Syrian Agricultural Settlement Zones (ASZs, which are classified based on several agro-ecological variables (annual rainfall depth and probability and geomorphological features) for policy and planning purposes since the early 1970s (IFAD 2010). The categories of the ASZs are given in the study (Ülker, Erguven, Gazioglu, 2018) as follows.

- ASZ 1: The most humid zone of Syria is divided into two areas: ASZ 1a: This area receives more than 600 mm of precipitation, and rainfed crops are productively planted. ASZ 1b: This area receives 350-600 mm precipitation and not less than 300 mm in two years out of three. Thus, it has the potential to get two seasons every three years. Wheat, legumes, and summer crops are the primary crops here.
- ASZ 2: A zone with annual precipitation of 250-350 mm and not less than 250 mm in two years out of three. The area is suitable for barley but also wheat, legumes, and summer crops. The usual rotation in this zone changes based on the depth of the soil. On deep soil, wheat pulses and forage legumes – a summer crop is planted if winter rain is adequate; otherwise, the summer crops will fall fallow. On shallow soil, primarily barley, but part of the land is planted with cumin. Thus, fallow is rarely carried out.
- ASZ 3: Precipitation of 250-300 mm and more than 250 mm in one year out of two. This zone is suitable for barley, the primary crop, and some legumes in the rotation could be planted. It is probable to get one to two seasons every three years. Fallow is practiced in the case of investment shortage.
- ASZ 4: These are marginal lands with 200-250 mm precipitation and not less than 200 mm during half the related years. Lands in this zone were used for growing barley or grazing, but cultivation is precarious and thus forbidden by law. Recent agricultural policy changes have affected this area: (1) Official credit does not exist for crop production because cropping is uncertain. (2) Fertilizer is not dedicated to rainfed

crops because it is unnecessary in this marginal zone. (3) Since it is a marginal production zone, not all farmers participate in the government production plan and hence do not have crop production licenses that authorize them to subsidize inputs. (4) Groundwater pumping to irrigate the summer crops is inhibited.

- ASZ 5: This is the desert and steppe area used only for grazing, with less than 200 mm precipitation. It is generally defined as steppe after excluding irrigated lands and marked as a Badia agro-ecological zone. It is a natural grazing area for sheep and camels (IFAD, 2010).

According to Global Trade Analysis Project (GTAP) (2005), the agro-ecological zones in Syria consist in 4 classes as (1) temperate arid, (2) temperate dry semi-arid, (3) temperate moist semi-arid, and (4) temperate sub-humid. The zones were mapped and given in Fig 3. In FAO (2018) special report for Syria, the country can be divided into the five Agro-Ecological Zones (AEZs) based on the level of annual precipitation received, as shown in Fig 4.

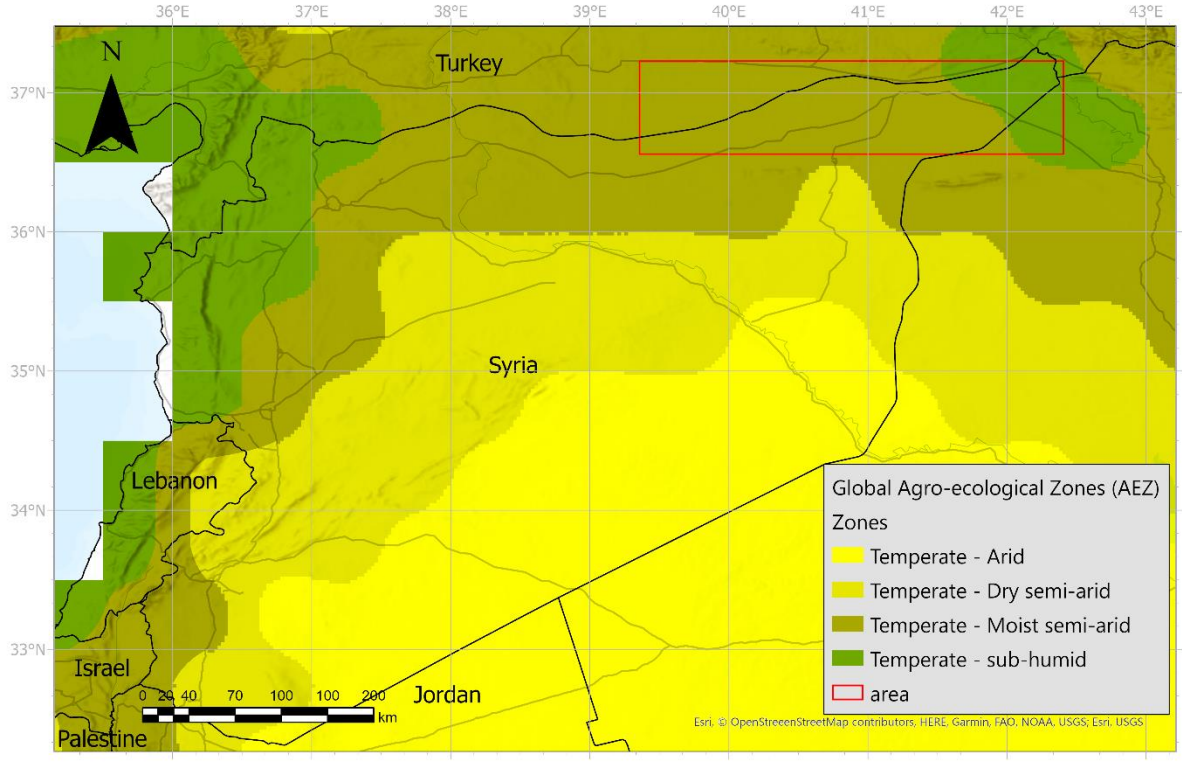


**Fig 3.** Agro-ecological zones in Syria (data source: GTAP, 2005; mapping by ArcGIS pro 2.8). Area indicates the study area (in legend).

Issue: 4 2022
Int. Journal of Water Management and Diplomacy
e-ISSN:2717-8277 Research Article

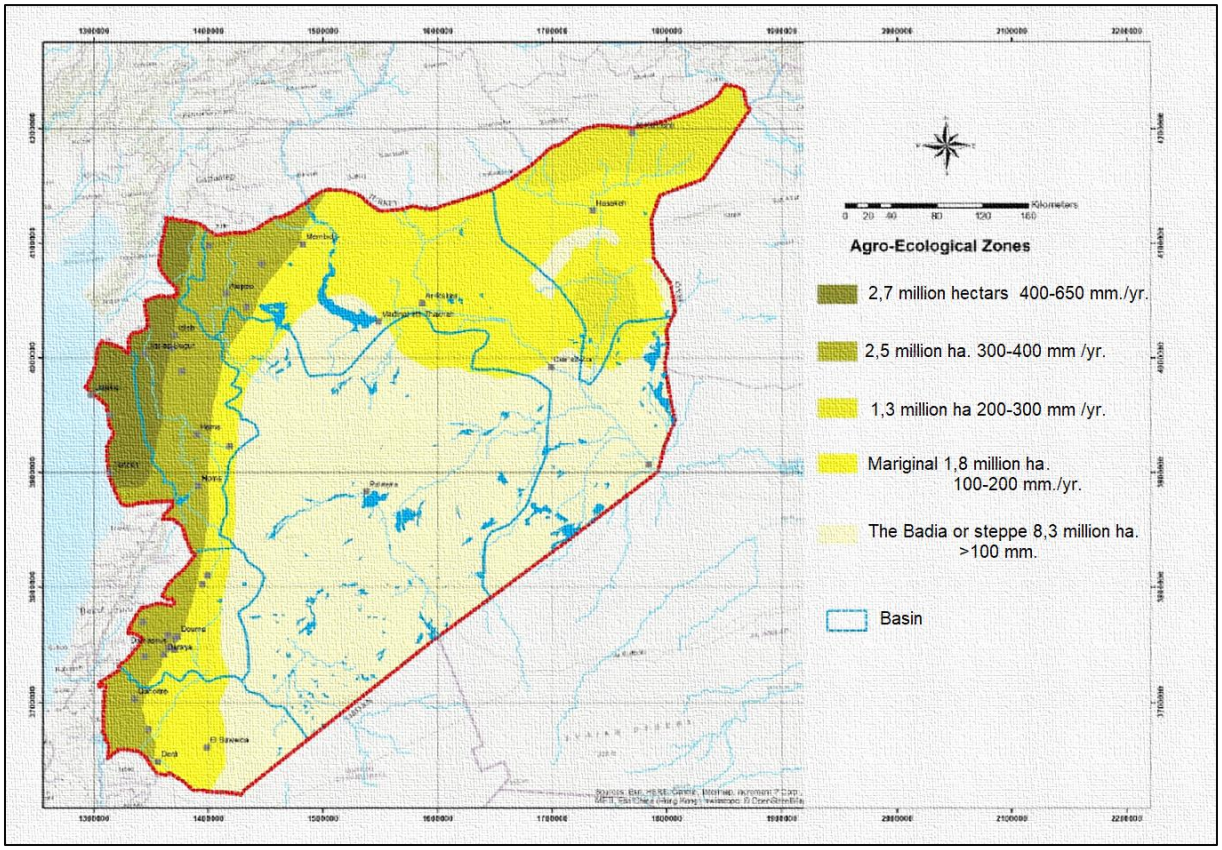


**Fig 4.** Agro-Ecological Zones (AEZs) are based on the level of annual precipitation (FAO, 2018).

### 1.1. Groundwater Use

Groundwater use in Syria has increased considerably and is overexploited in an unsustainable manner. Almost 60% of all irrigated sites in Syria depend on groundwater (Salman and Mualla 2004). Areas irrigated by groundwater increased by 140% from 1985 to 2002 (Somi, Zein, Dawood, Sayyed-Hassan, 2002).

About 87% of all water is used for irrigation, with almost 60% taken from groundwater resources, which leads to immense and unsustainable exploitation of these resources (Wada, Beek, Bierkens, 2012). The rest is used for household and industrial purposes, which account for 9% and 4%, respectively (Salman and Mualla 2004). Therefore, the highest water consumption can be detected in areas where irrigation is common. About 44% of water is consumed in the Euphrates & Aleppo basin, followed by Dejlah & Khabour. 33% of total groundwater wells were drilled in Al Hassake Region for irrigation, followed by Aleppo and Al Raqqa. These regions are responsible for almost 70% of groundwater pumping in total (Table 1). When dividing amounts of withdrawals by the area of each region, the Al Hassake region also accounts for the highest withdrawal per km$^2$ (Baba, Kareem, Yazdani, 2021).

**Table 1.** Data for drilled wells in Syria's region from FAO (2012).

| Region | Private Well | Government Project |
|---|---|---|
| Daar'a | 13075 | 20992 |
| Damascus | 44543 | - |
| Homs | 22655 | 27518 |
| Hama | 55798 | 7979 |
| Idleb | 44515 | 11164 |
| Aleppo | 101213 | 89358 |
| Al Raqqa | 51407 | 93128 |
| Deir Ezzor | 25420 | 38173 |
| Al Hassake | 313248 | - |

Al Hassake region also accounts for the highest number of drilled wells (313248), all private wells. (Table 1). About 300000 ha area is equipped for irrigation in the Al Hassake region, and 75% of this area is used groundwater. Almost 60% of all irrigated sites in Syria depend on groundwater. Areas that are irrigated by groundwater have increased each year. However, groundwater resources have been affected by natural and anthropogenic factors. Salinization is one of the critical problems for sustainable agricultural activity. This problem, which is of particular concern because it can limit socio-economic development in many areas, continues to attract scientists' attention to preserve and protect groundwater quality (Baba, Kareem, Yazdani, 2021).

In the Al Hassake region, mainly groundwater has been unsustainably exploited, which will worsen the situation quantitatively and qualitatively without recharge of resources. Due to over-pumping and the increase in unsustainable wells observed in recent decades, groundwater is quantitatively declining. Generally, groundwater contamination sources fall into two main categories: natural and anthropogenic sources. Significant sources of natural groundwater pollution include climate effects. For example, about 43% of groundwater has a high concentration of $SO_4$ and/or NaCl. This is particularly dominant in the eastern region of Syria due to the severe environment where rainfall is relatively low, and evaporation is high (Baba, Kareem, Yazdani, 2021). As seen in Fig 5, water in Syria has primarily used for irrigation, and nearly half of irrigation systems use groundwater as their main water resource (Salman and Mualla 2004).

Issue: 4 2022
Int. Journal of Water Management and Diplomacy
e-ISSN:2717-8277 Research Article

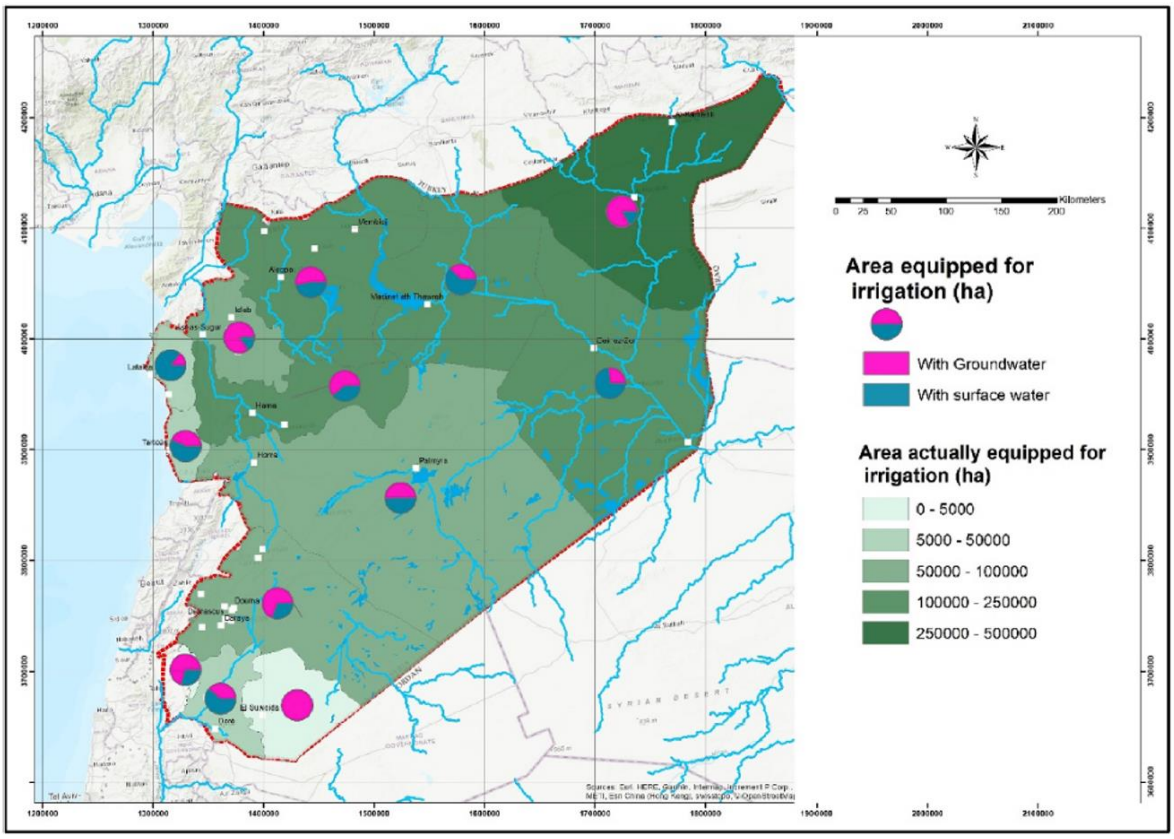


**Fig 5.** Area equipped for irrigation and irrigation resources (Mourad and Berndtsson 2012).

## 2. STUDY AREA

The study area lies in Northeast Syria (Fig 6 and Fig 7). North-east Syria is described as the land located on the right bank of the Euphrates River. It also consists of a small part of the catchment area of the neighbouring Tigris River. Generally, the terrain is low-lying, becoming hillier and less flat in the north. Elevation ranges from 200 to 500 **m**eters **a**bove **s**ea **l**evel (MASL). There is only one geological characteristic with higher elevation—the Abdel Aziz mountains, located parallel to the Sinjar in Iraq— specifying how this plate moved north and folded in the geological past, affecting the oil resources in the area (Graham, Muawia, Al-Maleh, Sawaf, 2001).

Demographic and community data vary according to the source and date. There are over three million people presently residing in northeast Syria (UNOCHA, 2019), including many Internally Displaced Persons (IDP) and imprisoned members of the Islamic State in large camps (ACAPS, 2020). The population is spread over major cities and many smaller towns and villages, as well as larger IDP camps.

Issue: 4 2022
Int. Journal of Water Management and Diplomacy
e-ISSN:2717-8277 Research Article

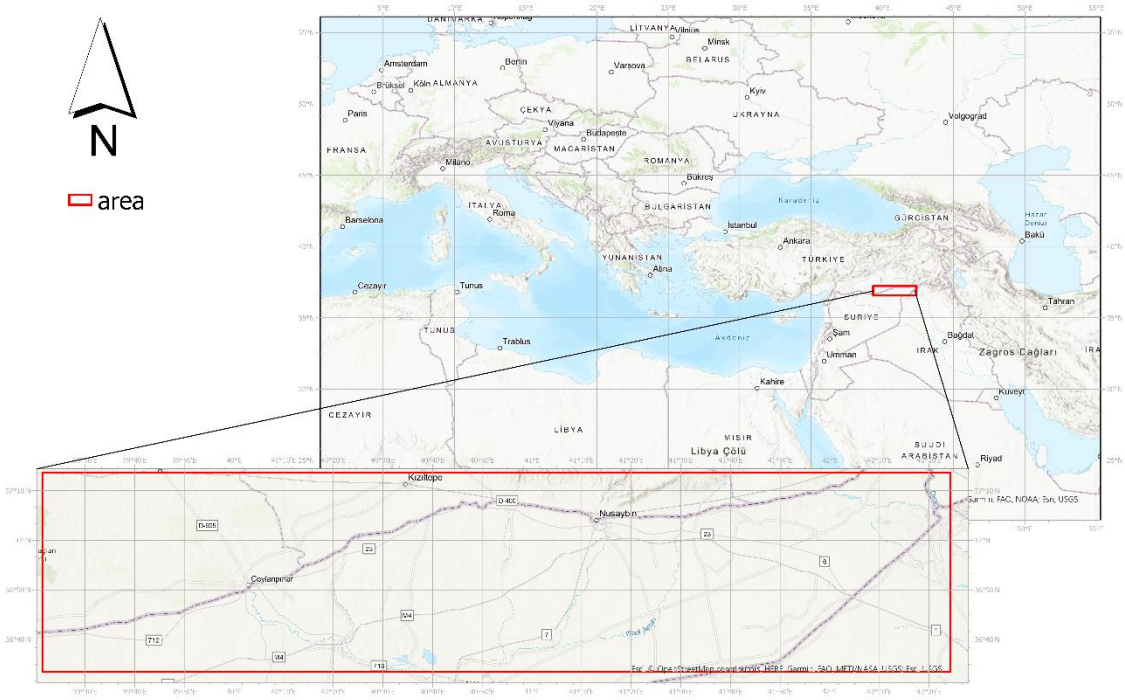


**Fig 6.** Locator map of the study area.

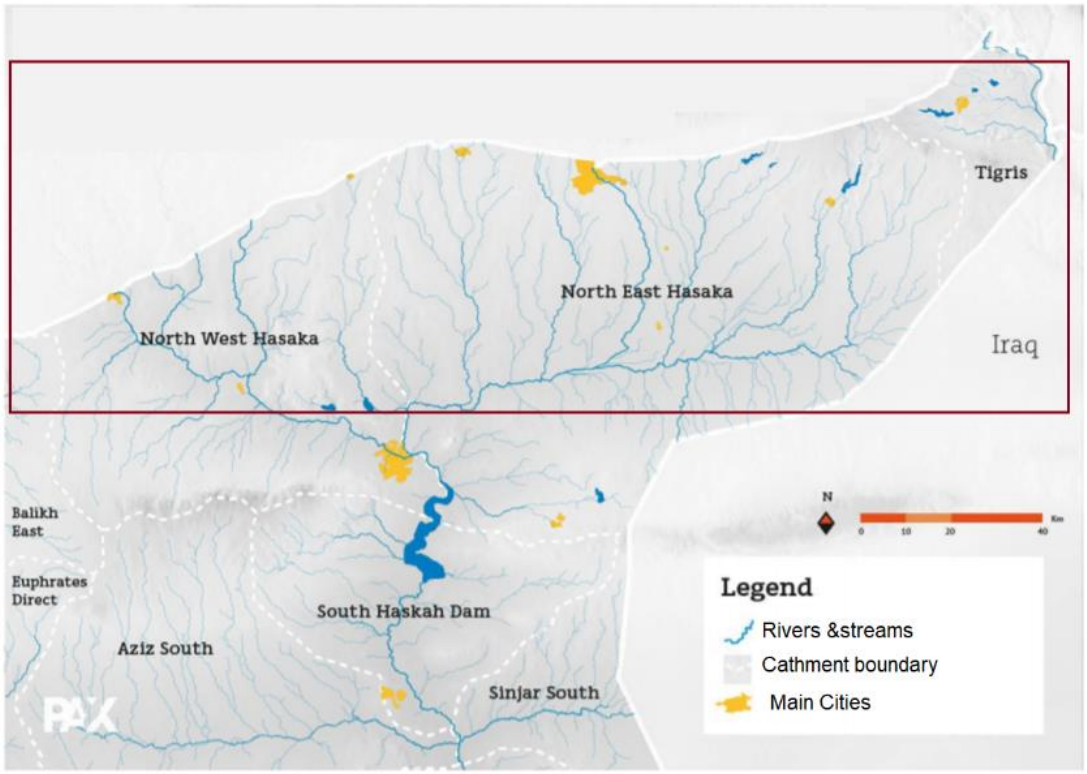


**Fig 7.** Study area in detail (Zwijnenburg, Nahas, Vasquez, 2021).

## 3. DATA AND METHOD

The selected study area includes (1) the Euphrates and Tigris basins of Southeast Turkey, (2) the Euphrates and Al-Khabour basins of North-east Syria, and (3) the Tigris basin of North-west Iraq. The study area is discussed in light of some parameters. These parameters are:

(1) Area equipped for irrigation (AEI-AI) with groundwater (AEI-Groundwater) or surface water (AEI-Surface water)
(2) Land use changes (LUCs)
(3) Spatio-temporal changes in shallow groundwater wetness percentile (GWS)
(4) Trends in precipitation
(5) Temporal changes in Standardized Precipitation-Evapotranspiration Index (SPEI)
(6) Timeline of conflicts

In this study, which presents the situation of Syria and neighbouring countries in the study area in detail, how much ground and surface water is used in the area equipped for irrigation has been revealed.

After determining which resource in the study area was mainly used, spatio-temporal land use changes in the region were examined. The change over the years was identified for each land-use class.

The temporal variation of the GWS values, which can be evaluated together with the examination of the LUCs in the region, has also been evaluated within the scope of this study.

The temporal variation of the precipitation parameter, which may affect the temporal variation of groundwater and other water resources in the region, has been determined in the study, and the long-term trend of SPEI values has also been revealed.

At the end of all these temporal change analyses, the relationship between LUC, GWS, and SPEI (potential measure of drought) changes with the trend of conflict events in the region are discussed.

### 3.2. Database Development for the Study

In this study, the Area Equipped for Irrigation data (AEI-Actually Irrigated (AI), AEI-Groundwater, and AEI-Surface water) was obtained from Intergovernmental Hydrological Program (Siebert, Henrich, Frenken, Burke, 2013; IHP-UNESCO, 2017; AQUASTAT-FAO, 2017) with 8.32 km spatial resolution and mapped in the ArcGIS Pro 2.8 environment. Area irrigated (AEI-AI) is a percentage of the area equipped for irrigation. The statistics with a reference year closest to the year 2005 were chosen for this version of the Global Map of Irrigation Areas.

The spatio-temporal land use/cover data were attained from Copernicus Climate Change Service's Land cover maps (2000 to 2020) with 300 m spatial resolution (Copernicus Climate Change Service, 2021). The database mentioned that the entire Medium Resolution Imaging Spectrometer (MERIS) Full and Reduced Resolution archive from 2003 to 2012 was first classified into a unique 10-year baseline land cover map. This is then back- and up-dated using change detected from (i) Advanced Very-High-Resolution Radiometer (AVHRR) time series from 1992 to 1999, (ii) SPOT-Vegetation (SPOT-VGT) time series from 1998 to 2012, and (iii)

PROBA-Vegetation (PROBA-V) and Sentinel-3 OLCI (S3 OLCI) time series from 2013. Copernicus Climate Change Service provides these maps' long-term consistency, yearly updates, and high thematic detail on a global scale (Copernicus Climate Change Service, 2021). In these maps, the typology was defined using the Land Cover Classification System (LCCS) developed by the United Nations (UN) Food and Agriculture Organization (FAO), with the view to be as much as possible consistent with the GLC2000, GlobCover 2005, and 2009 products. In addition, the UN-LCCS was found quite compatible with the Plant Functional Types (PFTs) used in climate models (ESA, 2017).

As a groundwater drought indicator, Shallow Groundwater Drought Indicator data (GWS) were obtained from the Nasa Grace database between 2003 and 2021 with 27.75 km spatial resolution (NASA Grace, 2021). NASA Grace documentation indicates that the groundwater indicator is based on terrestrial water storage observations derived from GRACE-FO satellite data and integrated observations. In Fig 8, the indicators describe current wet or dry conditions, showing the probability of occurrence with lower values (warm colors) meaning dryer than usual and higher values (blues) meaning wetter than usual.

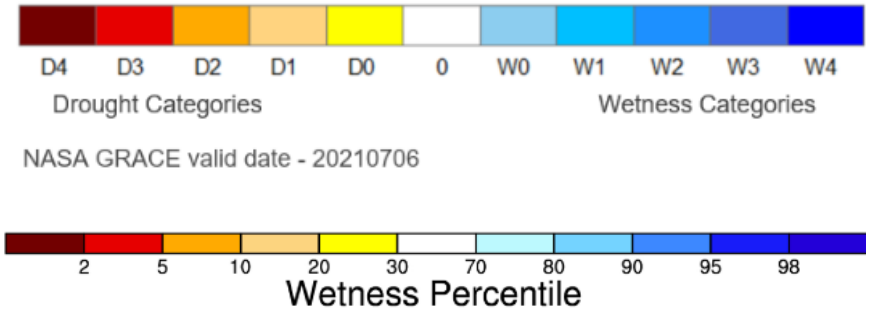


**Fig 8.** Wetness percentile classification (above) and percentile values (below) (NASA Grace 2021).

In this study, the Standardised Precipitation-Evapotranspiration Index (SPEI) was used to evaluate the drought conditions of the study area. SPEI data were attained from SPEI (2021) (https://soton.eead.csic.es/spei/index.html). The dataset is updated during the first days of the following month based on the most consistent and updated sources of climatic data. Mean temperature data are attained from the NOAA NCEP CPC GHCN_CAMS (for download; ftp://ftp.cpc.ncep.noaa.gov/wd51yf/GHCN_CAMS/) gridded dataset. Monthly precipitation totals data are obtained from the Global Precipitation Climatology Centre (GPCC) (for download; ftp://ftp-anon.dwd.de/pub/data/gpcc/first_guess/). The Climate Prediction Center (CPC) data with an original resolution of 55.5 km is interpolated to the resolution of 111 km (SPEI, 2021).

The SPEI Global Drought Monitor is currently based on the Thornthwaite equation for estimating **p**otential **e**vapo**t**ranspiration (PET). This is due to the lack of real-time data sources for computing more robust PET estimations with more extensive data requirements. The SPEI Global Drought Monitor is thus its near real-time character, a characteristic best suited for drought monitoring and early warning purposes (Begueria, Latorre, Reig, Vicente-Serrano, 2021).

e-ISSN:2717-8277 Research Article

## 4. RESULTS AND DISCUSSIONS

### 4.1. Relations of groundwater (GW) and surface water (SW) with the areas equipped for irrigation

Area equipped for irrigation and actually irrigated (AEI-AI), AEI-Groundwater, and AEI-Surface water were mapped by ArcGIS pro 2.8 software and shown in Fig 9, Fig 10, Fig 11.

In this study, the area equipped for irrigation (AEI) is considered separately for both groundwater (AEI-Groundwater) and surface water (AEI-Surface water). Therefore, it was calculated how much groundwater (GW) or surface water (SW) was used according to the irrigation percentages in the total irrigated area by the spatial analyses employed via ArcGIS pro 2.8. As a result, the graph shows the groundwater and surface water usage rates in irrigated areas in Fig 12.

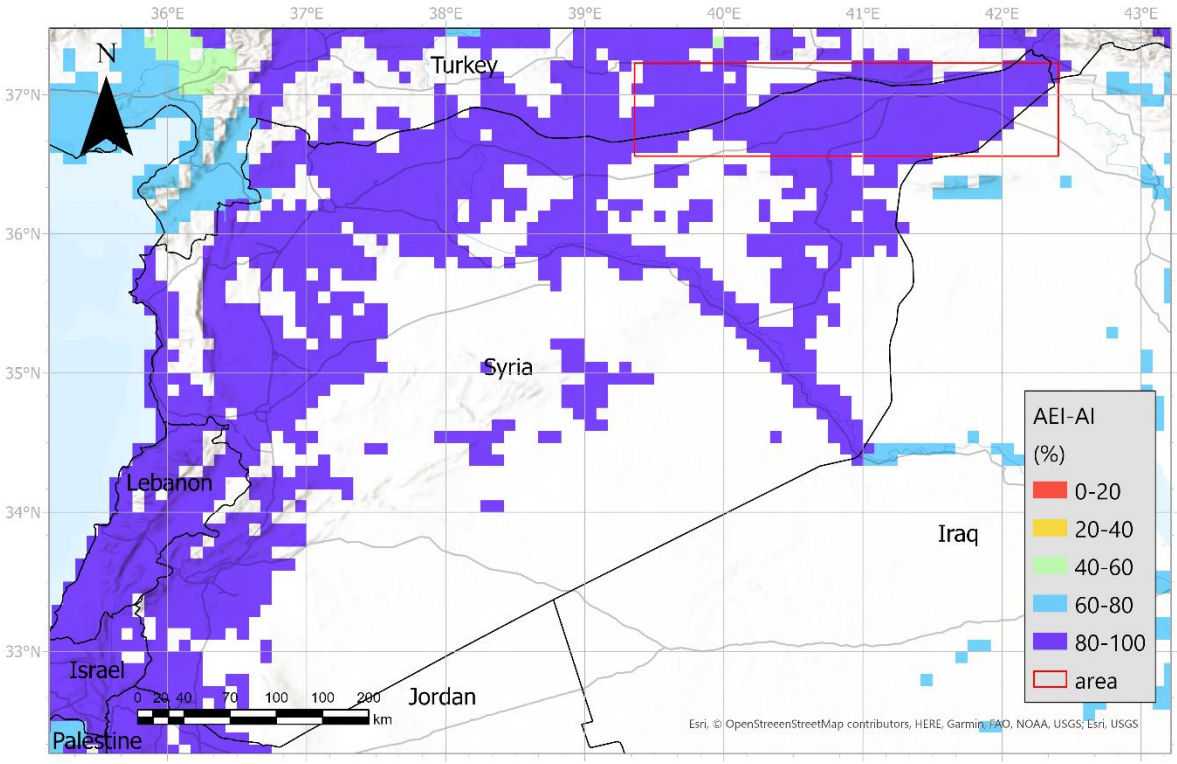


**Fig 9.** Area equipped for irrigation and actually irrigated (AEI-AI).

Issue: 4 2022
Int. Journal of Water Management and Diplomacy
e-ISSN:2717-8277
Research Article

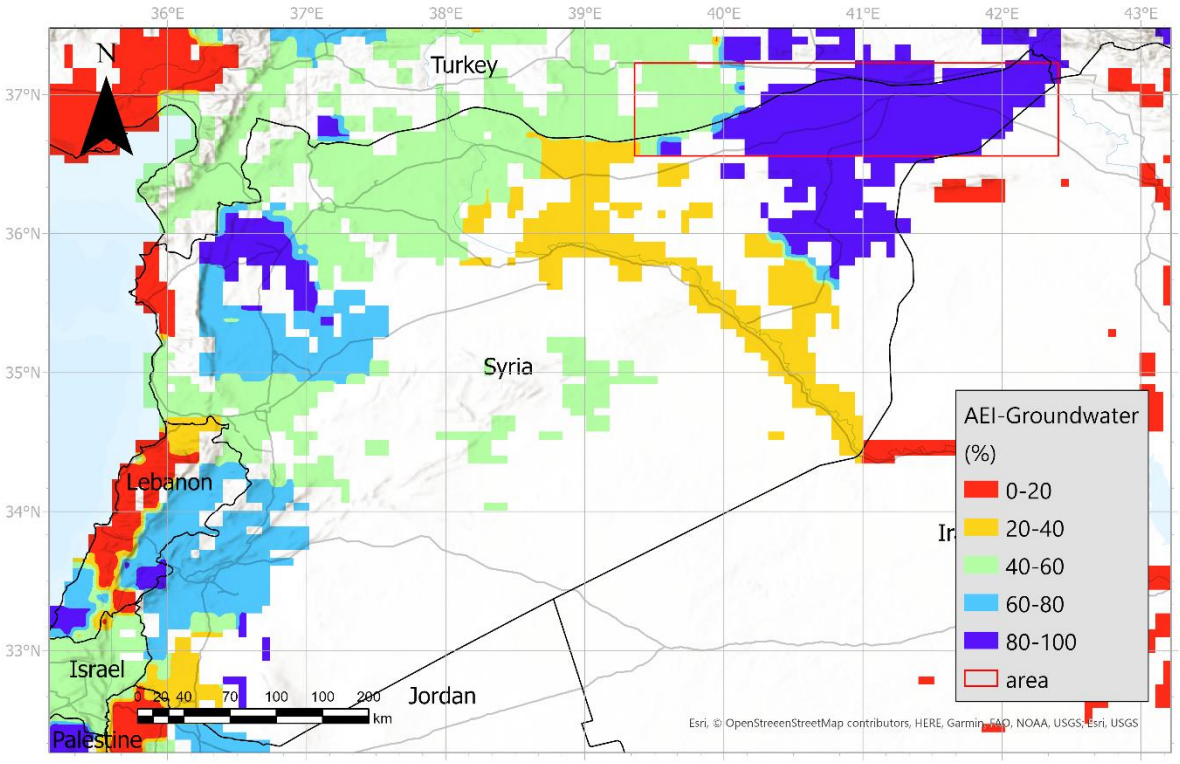


**Fig 10.** Area equipped for irrigation with groundwater (AEI-GW).

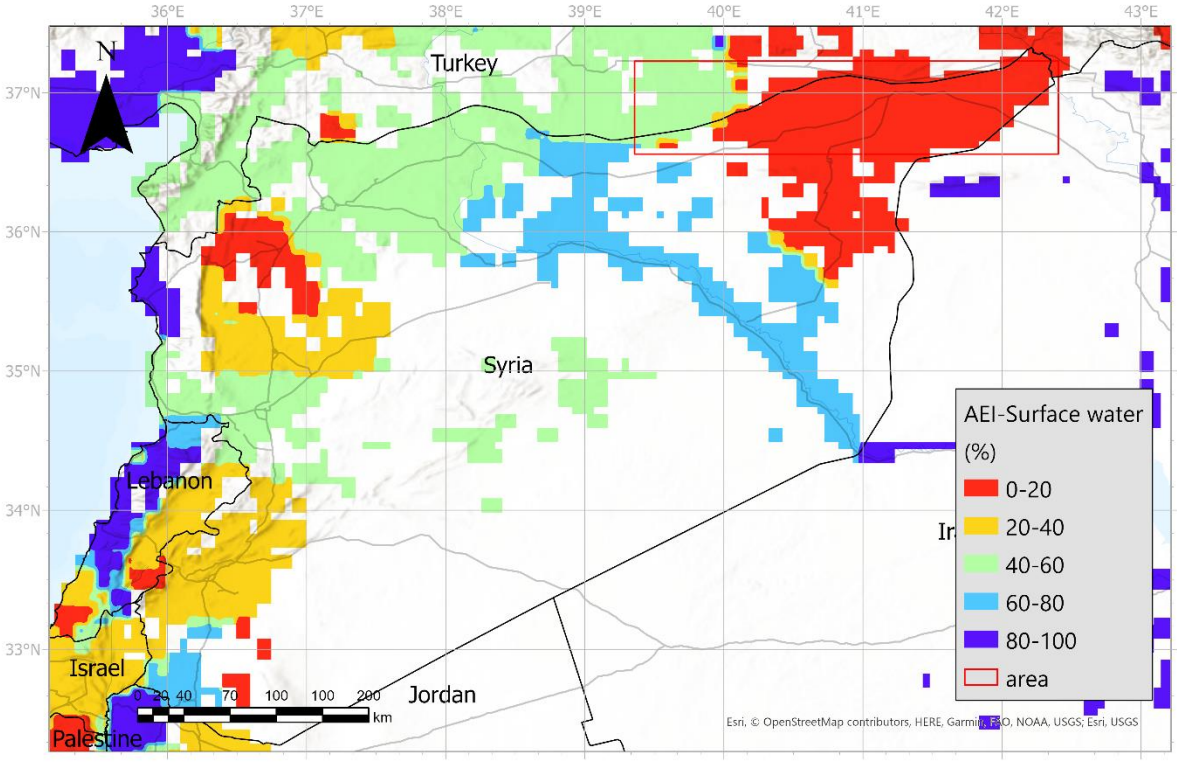

**Fig 11.** Area equipped for irrigation with surface water (AEI-SW).

As calculated from the data of Intergovernmental Hydrological Program, an area of approximately 76377 km² is irrigated in Syria (Fig 9). The actual irrigation rate of the irrigated areas in Syria is between 77.26% and 100%. The total of the irrigated areas between 80% and 100% is 76131 km². The area irrigated between 77.26% and 80% was determined as 246 km². GW and SW are used among the sources used for irrigation in these areas.

Areas with intensive groundwater irrigation are generally in the Al-Khabour water basin (Fig 1) in the north-east of Syria (Fig 10). When viewed transboundary in this region, groundwater use in Turkey is quite intense in regions equipped for irrigation and actually irrigated between 40% and 100%. However, Turkey also benefits from surface water in these regions (Fig 11). Apart from Al-Khabour, another region where groundwater is used intensively is the north of the Orontes water basin (Fig 1).

The study area, which is the focus of this study, is located within the Euphrates and Al-Khabour basins. While groundwater is used intensively in the Syrian part of the study area, both underground and surface water resources are utilized in the Turkish part of this area (Fig 10 and Fig 11).

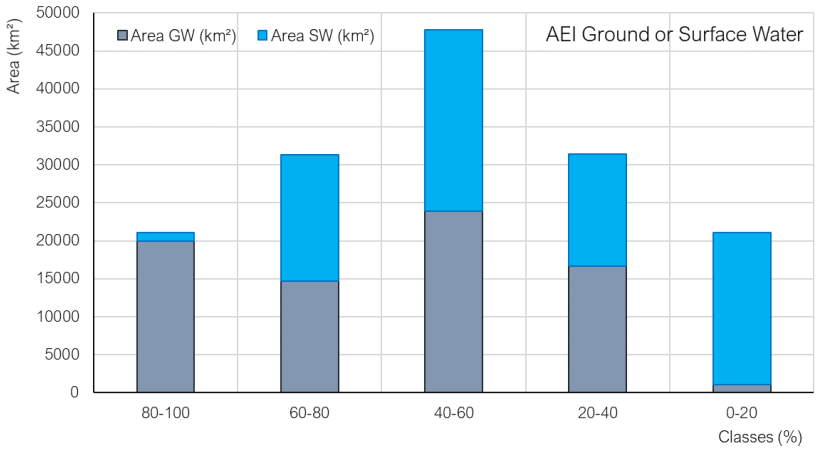


**Fig 12.** Groundwater and surface water usage rates in the areas equipped for irrigation.

As shown in Fig 12, groundwater is predominantly used where 80% to 100% of the area equipped for irrigation is actually irrigated. In areas where irrigation is actually between 20% and 80%, groundwater and surface water are used almost equally. A large amount of surface water is used in areas where irrigation is really low (0-20%) of the area equipped for irrigation.

### 4.2. Spatio-temporal changes in land use

The study examined the change of land use classes in the region between 2000 and 2020. The change in agricultural areas is particularly remarkable. Here, agricultural areas are divided into two classes as irrigated and rainfed areas. The land use maps of 20 years between 2000 and 2020 are given in Fig 13 and Fig 14, respectively. Additionally, the detailed information about the legend used in the maps is given in Table 2.

Issue: 4 2022
Int. Journal of Water Management and Diplomacy
e-ISSN:2717-8277 Research Article

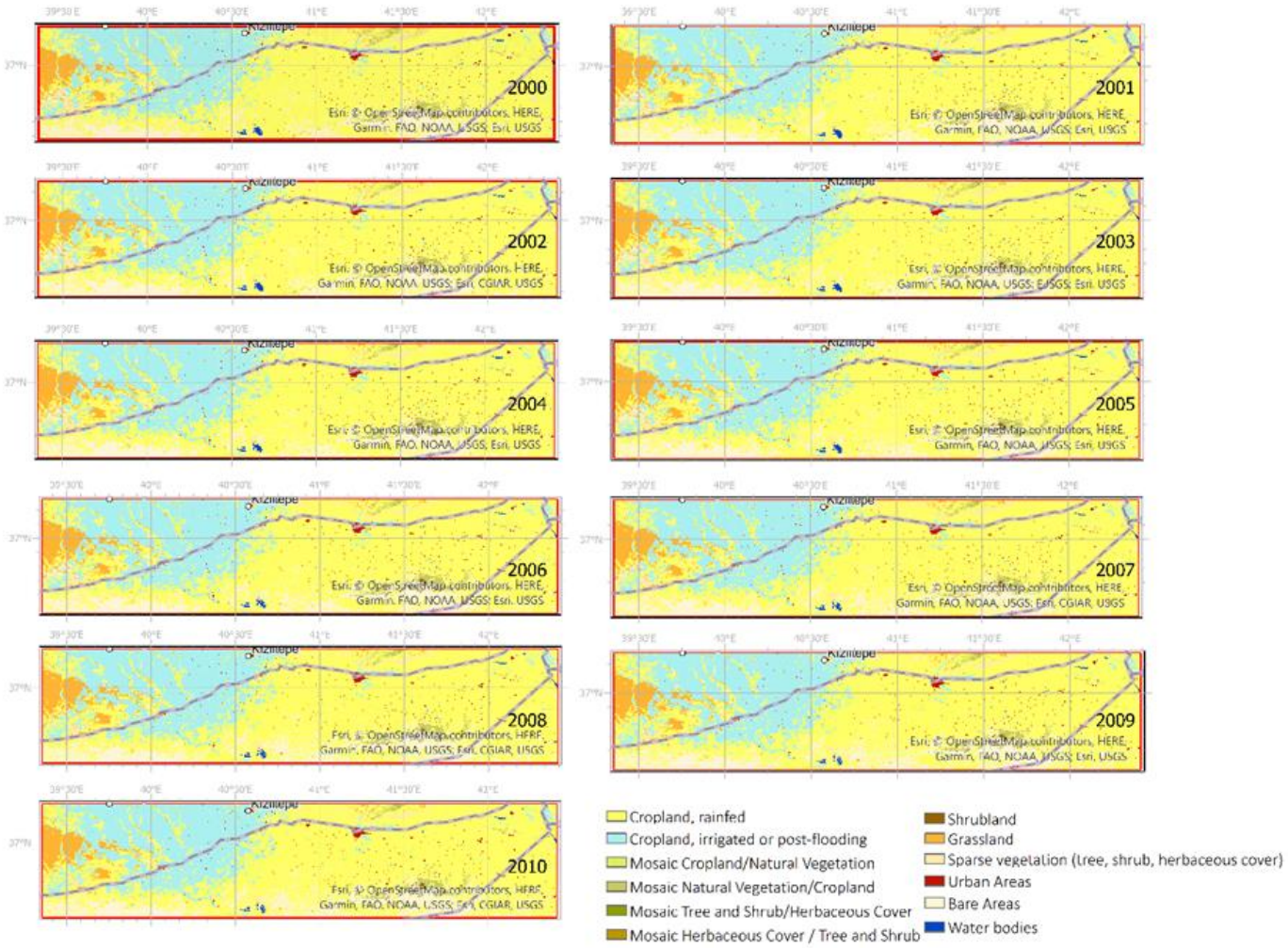


**Fig 13.** Land use classification maps from 2000 to 2010.

Issue: 4 2022
Int. Journal of Water Management and Diplomacy
e-ISSN:2717-8277 Research Article

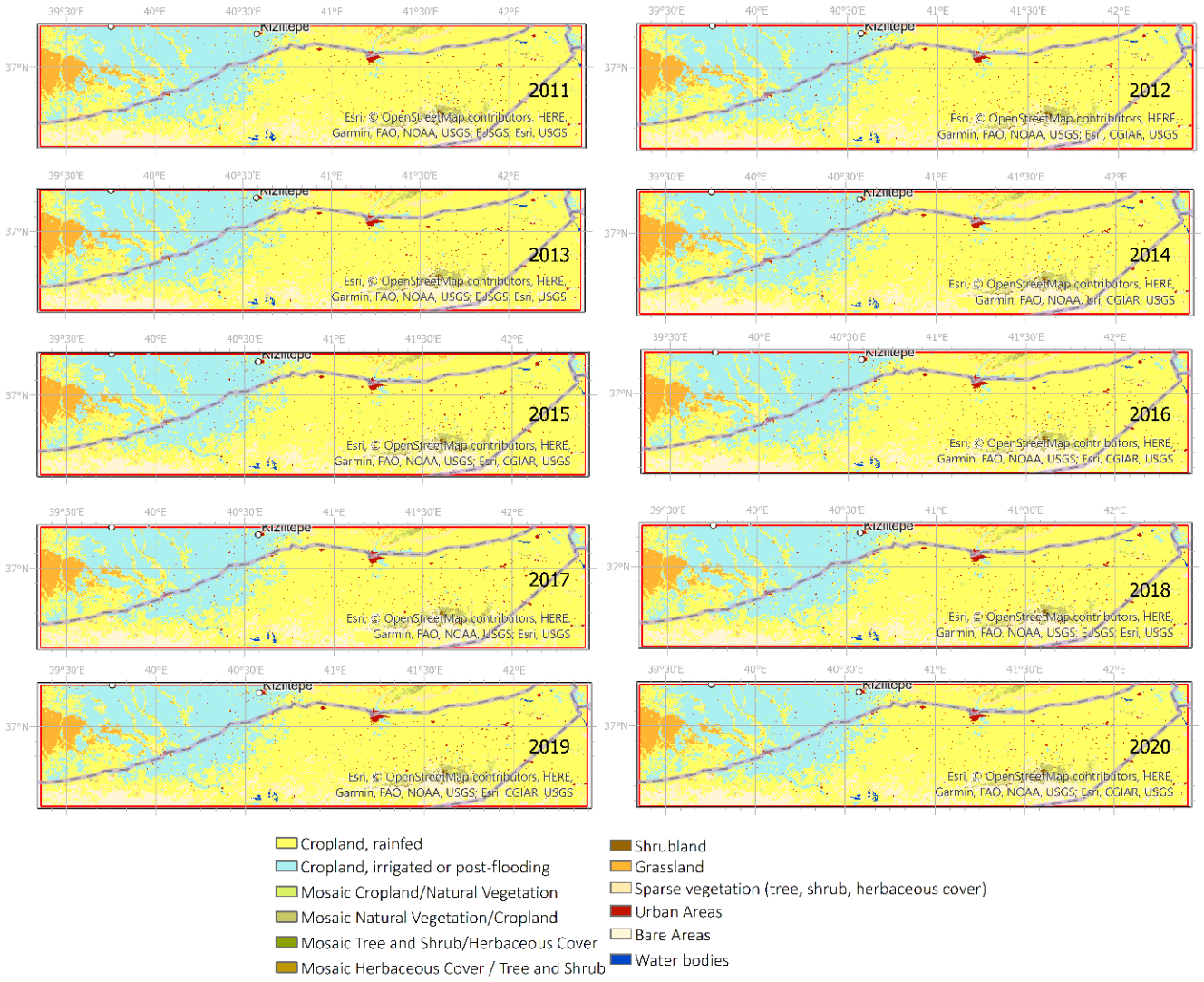


**Fig 14.** Land use classification maps from 2011 to 2020.

**Table 2.** Correspondence between the IPCC land categories used for the change detection and the LCCS legend used in the land cover classification maps (Fig 13 and Fig 14) (Copernicus Climate Change Service, 2021).

| IPCC Classes considered for the change detection | LCCS legend used in land cover classification maps |
|---|---|
| Agriculture | Rainfed cropland |
| | Irrigated cropland |
| | Mosaic cropland (>50%) / natural vegetation (tree, shrub, herbaceous cover) (<50%) |
| | Mosaic natural vegetation (tree, shrub, herbaceous cover) (>50%) / cropland (< 50%) |
| Forest | Mosaic tree and shrub (>50%) / herbaceous cover (< 50%) |
| Grassland | Mosaic herbaceous cover (>50%) / tree and shrub (<50%) |
| | Grassland |
| Shrubland | Shrubland |
| Sparse vegetation | Sparse vegetation |
| Settlement | Urban |
| Bare area | Bare areas |
| Water | Water |

The land use maps in Fig 13 and Fig 14 were also subjected to spatial change analysis in ArcGIS Pro 2.8. Particularly the temporal variations in the areas of (1) cropland (irrigated or post-flooding), (2) cropland (rainfed), (3) mosaic cropland/natural vegetation, and (4) mosaic natural vegetation/cropland were given between Fig 15 and Fig 16. The changes of all land use classes in the study area were also shown in Table 3.

It is also critical to determine the trend of land use change in Turkey and Syria. The extent of the change in especially irrigated and rainfed agricultural areas should be assessed by considering the two countries separately. Also, the change of urban areas over time should be evaluated individually for both countries. The study examined the spatio-temporal change of agricultural and urban areas by country, and the results were given in Table 4 and Fig 17.

Issue: 4 2022
Int. Journal of Water Management and Diplomacy
e-ISSN:2717-8277 Research Article

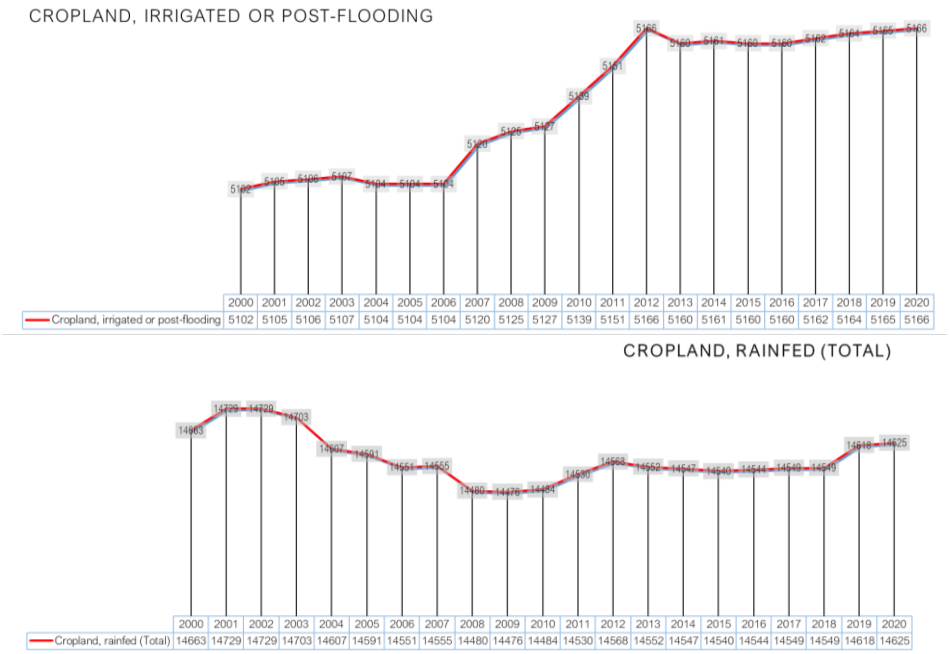


**Fig 15.** Spatio-temporal change (km²) of irrigated cropland and rainfed croplands between 2000 and 2020.

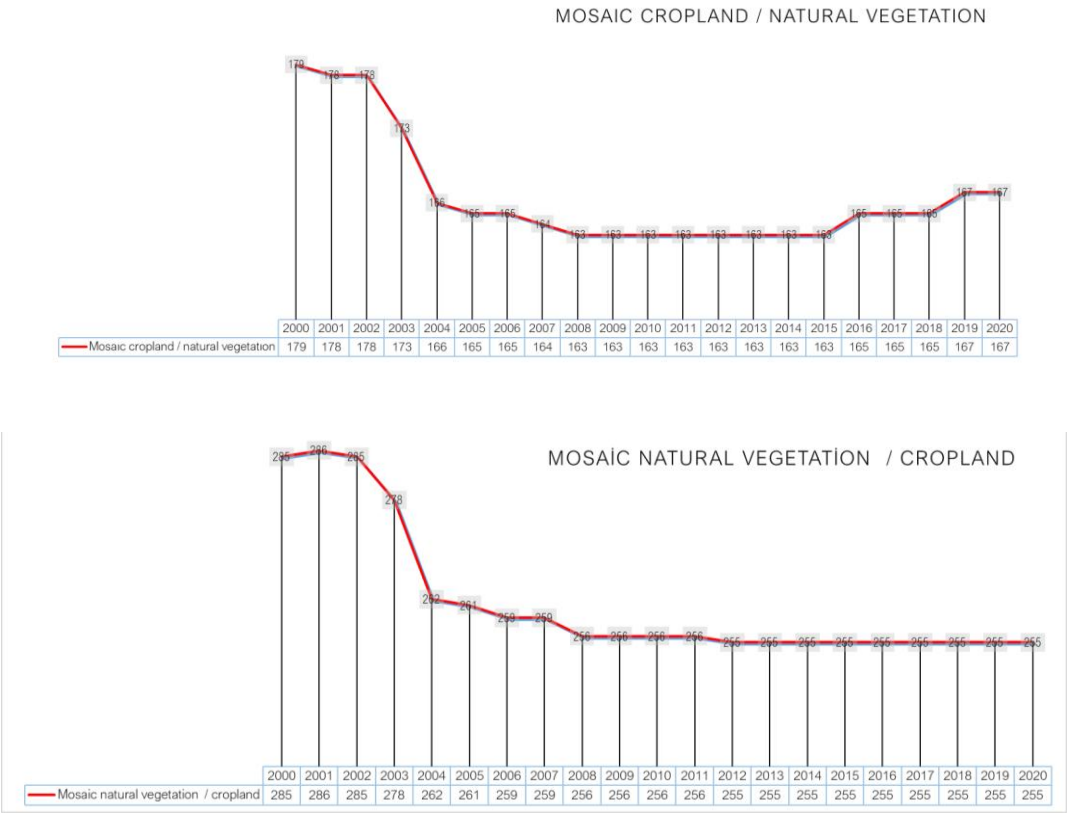


**Fig 16.** Spatio-temporal change (km²) of mosaic cropland/natural vegetation and mosaic natural vegetation/cropland between 2000 and 2020.

Issue: 4 2022
Int. Journal of Water Management and Diplomacy
e-ISSN:2717-8277 Research Article

**Table 3.** The area (km²) of LULC classes except agricultural areas (classes are based on IPCC classification).

| LULC Classes | 2000 | 2001 | 2002 | 2003 | 2004 | 2005 | 2006 | 2007 | 2008 | 2009 | 2010 | 2011 | 2012 | 2013 | 2014 | 2015 | 2016 | 2017 | 2018 | 2019 | 2020 |
|---|---|---|---|---|---|---|---|---|---|---|---|---|---|---|---|---|---|---|---|---|---|
| Mosaic tree and shrub/herbaceous cover | 2 | 2 | 2 | 2 | 2 | 2 | 2 | 2 | 2 | 2 | 2 | 2 | 2 | 2 | 2 | 2 | 2 | 2 | 2 | 2 | 2 |
| Mosaic herbaceous cover/tree and shrub | 1 | 1 | 1 | 1 | 1 | 1 | 1 | 1 | 1 | 1 | 1 | 1 | 1 | 1 | 1 | 1 | 1 | 1 | 1 | 1 | 1 |
| Shrubland | 26 | 26 | 26 | 26 | 26 | 26 | 26 | 26 | 26 | 26 | 26 | 26 | 26 | 26 | 26 | 26 | 26 | 26 | 26 | 26 | 26 |
| Grassland | 777 | 777 | 778 | 796 | 827 | 827 | 828 | 823 | 822 | 815 | 801 | 738 | 715 | 715 | 713 | 713 | 708 | 699 | 691 | 689 | 686 |
| Sparse vegetation (Total) | 453 | 397 | 391 | 396 | 416 | 420 | 424 | 401 | 397 | 390 | 364 | 362 | 336 | 341 | 341 | 341 | 341 | 343 | 343 | 335 | 335 |
| Urban areas | 166 | 167 | 167 | 167 | 167 | 167 | 168 | 168 | 170 | 171 | 172 | 174 | 176 | 180 | 187 | 195 | 195 | 196 | 201 | 201 | 201 |
| Bare areas | 2090 | 2075 | 2080 | 2095 | 2168 | 2182 | 2220 | 2230 | 2309 | 2323 | 2343 | 2348 | 2342 | 2356 | 2355 | 2355 | 2355 | 2355 | 2355 | 2293 | 2289 |
| Water bodies | 51 | 51 | 51 | 50 | 50 | 49 | 47 | 46 | 45 | 45 | 45 | 44 | 42 | 42 | 42 | 42 | 42 | 42 | 42 | 42 | 42 |

JWMD Issue: 4 2022
Int. Journal of Water Management and Diplomacy
e-ISSN:2717-8277 Research Article

**Table 4.** Spatio-temporal change (km²) for the agricultural areas (as Cropland, rainfed and Irrigated cropland) and urban areas in Turkish and Syrian parts of the study area.

| **LULC Classes** | **2000** | **2001** | **2002** | **2003** | **2004** | **2005** | **2006** | **2007** | **2008** | **2009** | **2010** | **2011** | **2012** | **2013** | **2014** | **2015** | **2016** | **2017** | **2018** | **2019** | **2020** |
|---|---|---|---|---|---|---|---|---|---|---|---|---|---|---|---|---|---|---|---|---|---|
| Turkey - Cropland, rainfed | 2727 | 2731 | 2736 | 2726 | 2708 | 2708 | 2707 | 2736 | 2757 | 2780 | 2816 | 2870 | 2906 | 2906 | 2903 | 2901 | 2904 | 2911 | 2914 | 2914 | 2916 |
| Syria - Cropland, rainfed | 10181 | 10211 | 10205 | 10189 | 10128 | 10114 | 10075 | 10051 | 9985 | 9959 | 9931 | 9922 | 9922 | 9906 | 9905 | 9901 | 9901 | 9900 | 9898 | 9936 | 9939 |
| Turkey - Cropland, irrigated or post-flooding | 3577 | 3579 | 3580 | 3580 | 3577 | 3577 | 3577 | 3593 | 3598 | 3601 | 3616 | 3629 | 3644 | 3647 | 3647 | 3647 | 3647 | 3649 | 3651 | 3652 | 3653 |
| Syria - Cropland, irrigated or post-flooding | 1486 | 1486 | 1486 | 1488 | 1488 | 1488 | 1488 | 1488 | 1488 | 1487 | 1484 | 1483 | 1483 | 1474 | 1474 | 1474 | 1474 | 1474 | 1474 | 1475 | 1474 |
| **Urban Areas** | **2000** | **2001** | **2002** | **2003** | **2004** | **2005** | **2006** | **2007** | **2008** | **2009** | **2010** | **2011** | **2012** | **2013** | **2014** | **2015** | **2016** | **2017** | **2018** | **2019** | **2020** |
| Turkey | 36 | 36 | 36 | 36 | 36 | 37 | 37 | 37 | 37 | 37 | 38 | 39 | 39 | 40 | 44 | 47 | 47 | 47 | 50 | 50 | 50 |
| Syria | 119 | 119 | 119 | 119 | 119 | 120 | 120 | 121 | 121 | 122 | 123 | 124 | 125 | 127 | 129 | 133 | 133 | 134 | 136 | 136 | 136 |

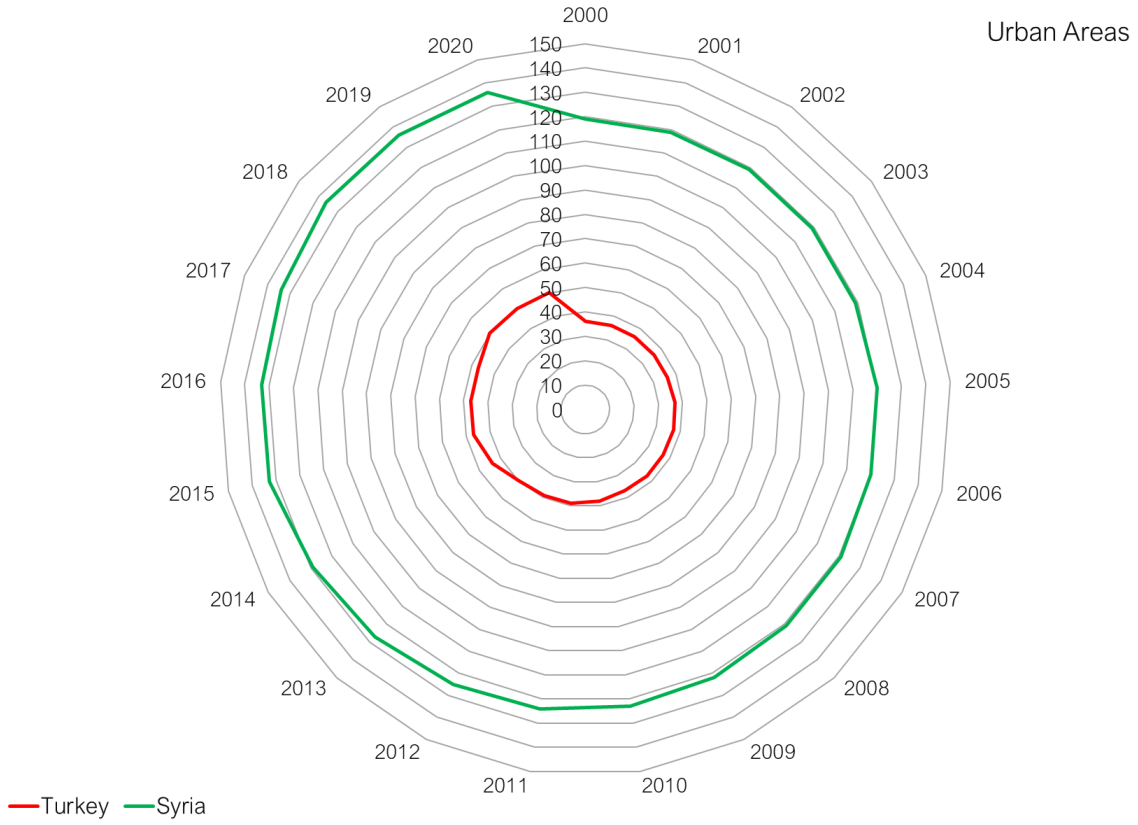


**Fig 17.** The spatio-temporal change (km²) of urban areas between 2000 and 2020 in Turkish and Syrian parts of the study area.

In Fig 15, irrigated agricultural areas experienced a significant increase, especially in 2006. These areas reached their maximum in 2012 (5166 km²), and there was no dramatic decrease until 2020. While rainfed agriculture had the largest area in the region between 2000-2004, it decreased after 2004. This spatio-temporal change shows the transition of the local communities' agricultural activities from rainfed agriculture to irrigated agriculture in the region. According to the 2005 "area equipped for irrigation data" in Fig 9, Fig 10 (GW), and Fig 11 (SW), the study area has the highest percentage of the irrigated area according to all Syrian lands. It was determined that this region, which had an irrigation capacity of 80% to 100% in 2005, switched to a high amount of irrigated agriculture in 2006. According to these assessments, local communities used more water in agricultural activities. The spatio-temporal change of mosaic cropland/natural vegetation and mosaic natural vegetation/cropland classes in Fig 16 shows the decrease in these areas as shifting to irrigated agriculture.

When countries are considered separately in Table 4, it has been determined that the area of rainfed agriculture in the region has increased over time in Turkey. However, this increase was reversed in some years (2003-2006 and 2014-2016). In the Syrian part, there was a decrease in the rainfed agricultural areas. Although there was an increase between 2000 and 2002, a decline was determined in rainfed agriculture from 2002 to 2018. In 2019 and 2020, a relative rise was observed.

In irrigated agriculture, an expansion has been determined in Turkey (Table 4). Although there was a decline in the irrigated agricultural areas between 2004-2006, the general trend is to increase the irrigated agriculture every year, albeit a little. In Syria, irrigated agricultural areas expanded between 2000-2008; however, after 2008, there has been a slight decrease in irrigated agricultural areas every year. The urban area expansion shows an increasing trend for both countries (Table 4 and Fig 17).

### 4.3. Historical GWS Change

In Fig 18, spatio-temporal GWS values were assessed in the study area. Although it was observed that the groundwater was high between 2003 and 2007; however, a significant decrease occurred in 2008 and 2009. This is consistent with the data in Fig 9 and Fig 10. The percentage of irrigated areas in the region in 2005 was relatively high compared to other parts of Syria (Fig 9). Additionally, irrigation is employed by groundwater intensively in this region (Fig 10). According to these data obtained in 2005 (Fig 10), it is inevitable that there will be a significant groundwater withdrawal after 2005.

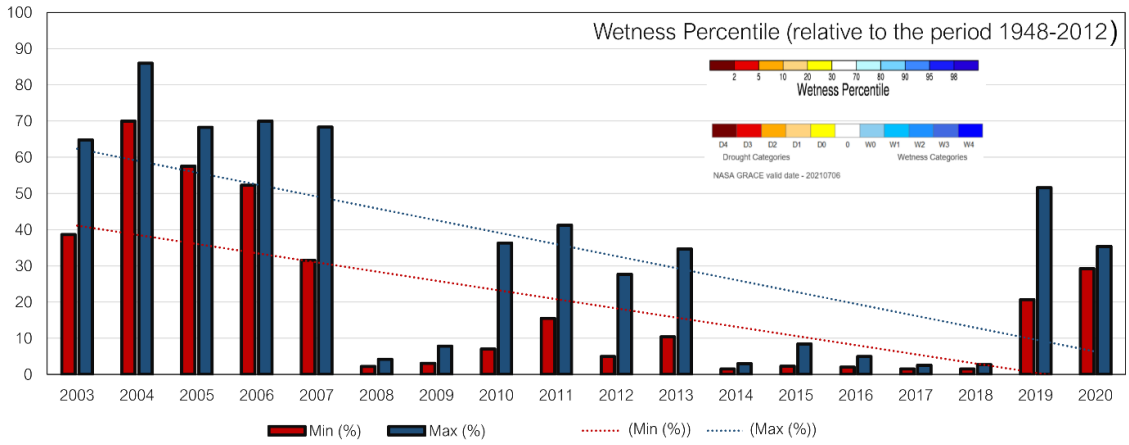


**Fig 18.** GRACE-Based Shallow Groundwater's wetness percentile (GWS) changes between 2003 and 2020.

The results in Fig 18 supports Fig 10. After 2007, groundwater has never regained its pre-2007 values. Compared to Table 4, the decrease in irrigated agriculture in Turkey between 2004-2006 and Syria's increase in irrigated agricultural areas in this period (2000-2008) explains the dramatic return of the high groundwater value between 2003-2007 in 2008-2009. Even though Syria decreased the irrigated agricultural areas, especially after 2009, Turkey's expanded irrigated agricultural areas caused the short-term increase in 2010-2013 not to continue, and a much more impressive decrease occurred between 2014-2018. Between 2019 and 2020, there was an increase in intensity in the groundwater level, even if the groundwater rates were not in 2007 and before.

### 4.4. Precipitation in the region and SPEI Results

Monthly precipitation and long-term average precipitation (1981-2010) near the Al-Hassake region, where lies our study area, is given in Fig 19. This figure shows that no precipitation has occurred in 5 months (July to November) between (1981-2010).

Issue: 4 2022
Int. Journal of Water Management and Diplomacy
e-ISSN:2717-8277
Research Article

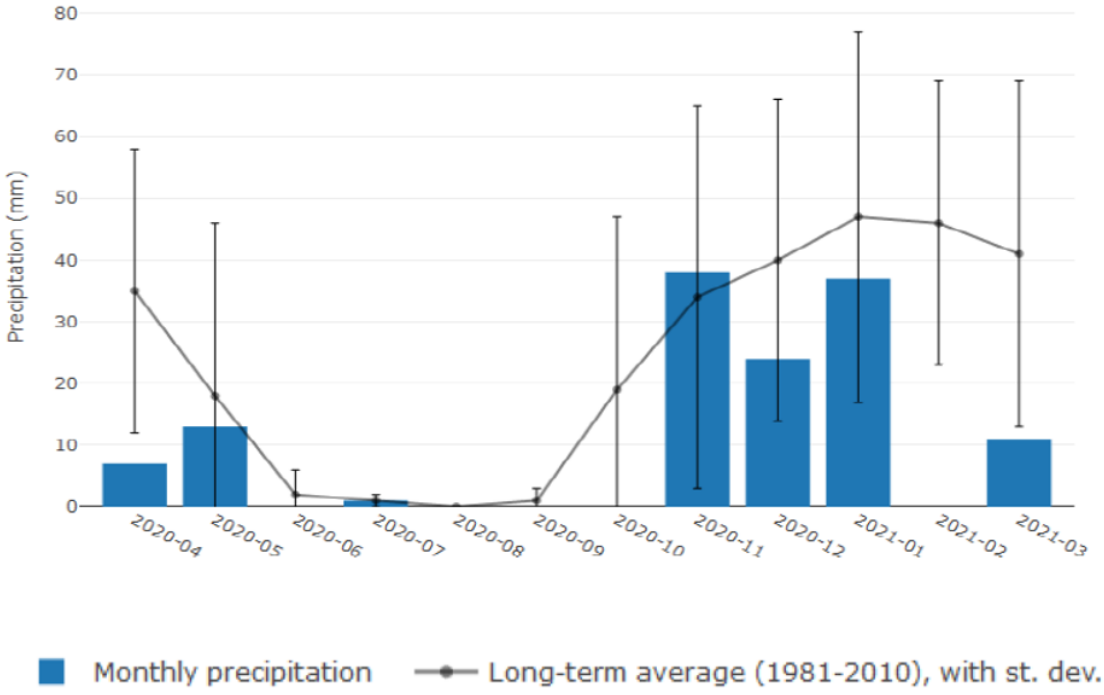


**Fig 19.** Monthly total precipitation near Al-Hassake, Syria (coordinates: 36.4°N, 40.7°E), with the long-term monthly average and standard deviation (1981-2010) (GDO, 2021).

The map of Fig 20 shows Standardized Precipitation Index (SPI) at the 6-month accumulation period, encompassing all the typically rainiest months of the year, hence emphasizing the areas that accumulated the highest precipitation deficit since autumn 2020, compared to the long-term average. As a result, most of Syria, the north of Iraq, and neighbouring Iranian and Turkish areas display meteorological drought. The index is significant, especially considering the role of precipitation anomalies at such a critical stage for the annual water balance (GDO, 2021).

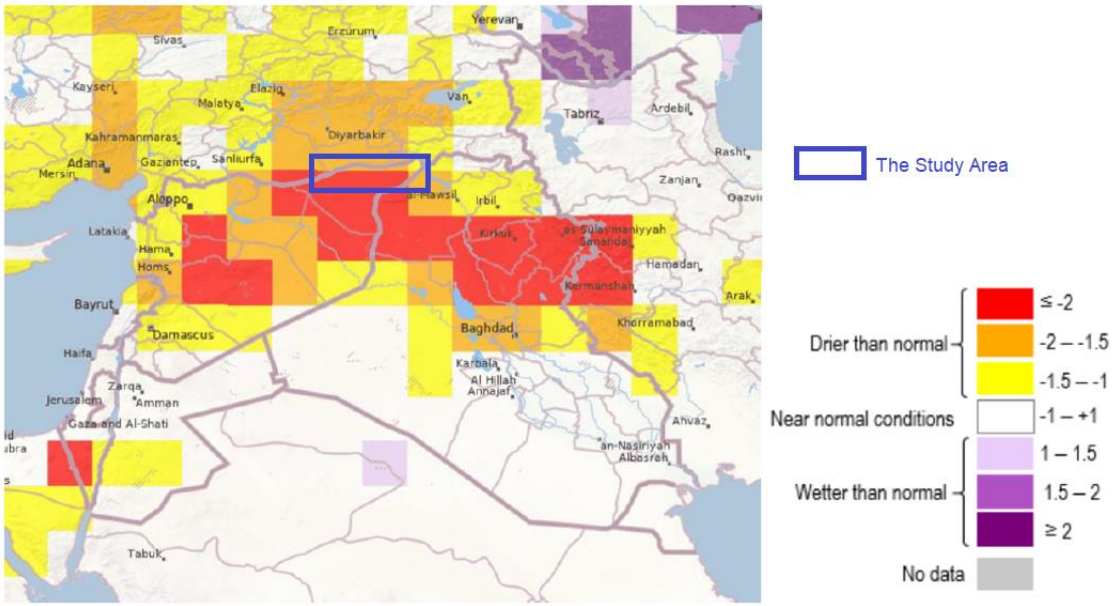

**Fig 20.** The anomaly of precipitation for October 2020 to March 2021 (SPI-6) over Syria and Iraq (GDO. 2021).

The charts in Fig 21 describe the downwards trend of precipitation anomalies in the past few months employing SPI-6 and SPI-12. The former demonstrates the overall decrease as precipitation totals stood well below a typical month after month since October 2020. The latter indicates that the consistent rainfall surplus was progressively depleted, and the annual balance was strongly negative. Thus, despite the high frequency of meteorological droughts in the past 25 years, the recent drought stands out as one of the worst over the same period (GDO, 2021).

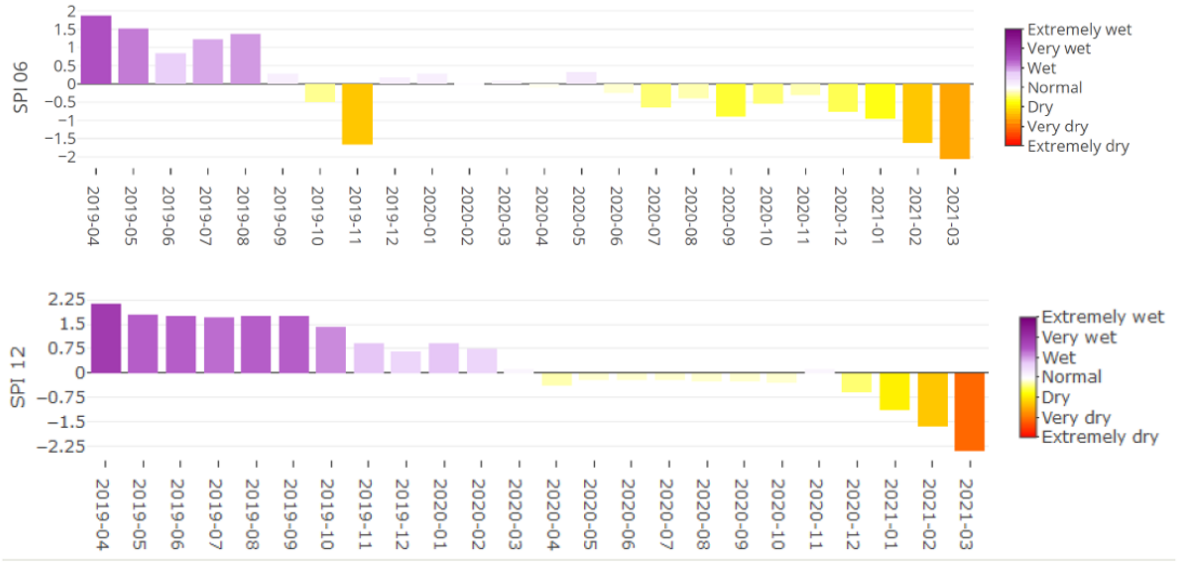


**Fig 21.** SPI for a cumulative period of 6 and 12 months near Al-Hassake (top and middle respectively, Al- Hassake, Syria (coordinates: 36.49°N, 40.74°E)) (GDO, 2021).

### 4.4.1. SPEI Results

The SPEI realizes the needs of a drought index since its multi-scalar nature enables it to be used by various scientific disciplines to detect, monitor, and analyse droughts. Like the Self-Calibrated Palmer Drought Severity Index (sc-PDSI) and the SPI, the SPEI can measure drought severity according to its intensity and duration and identify the onset and end of drought episodes. In addition, the SPEI allows the comparison of drought severity through time and space since it can be calculated over a wide range of climates, as can the SPI. Furthermore, Keyantash and Dracup (2002) indicated that drought indices must be statistically robust and easily calculated and have a clear and logical calculation procedure. The SPEI meets all these requirements. However, a crucial benefit of the SPEI over other broadly used drought indices that consider the effect of PET on drought severity is that its multi-scalar characteristics allow the recognition of different drought types and impacts in the context of global warming.

According to Lopez-Moreno and others (2013), three main sub-basin groups were distinguished based on the correlation of their streamflow responses to different time scales of the SPEI: (1) sub-basins correlated with short SPEI time scales (2–4 months), which generally corresponded to unregulated headwater areas; (2) sub-basins correlated with long

SPEI time scales (10–20 months), where groundwater reserves play a significant hydrological role; and (3) sub-basins correlated with medium SPEI time scales (6–10 months).

In this study, the SPEI results were given for 12 and 48 months in Fig 22 and Fig 23. The coordinates of the pixels in the study area are considered when dealing with the SPEI values.

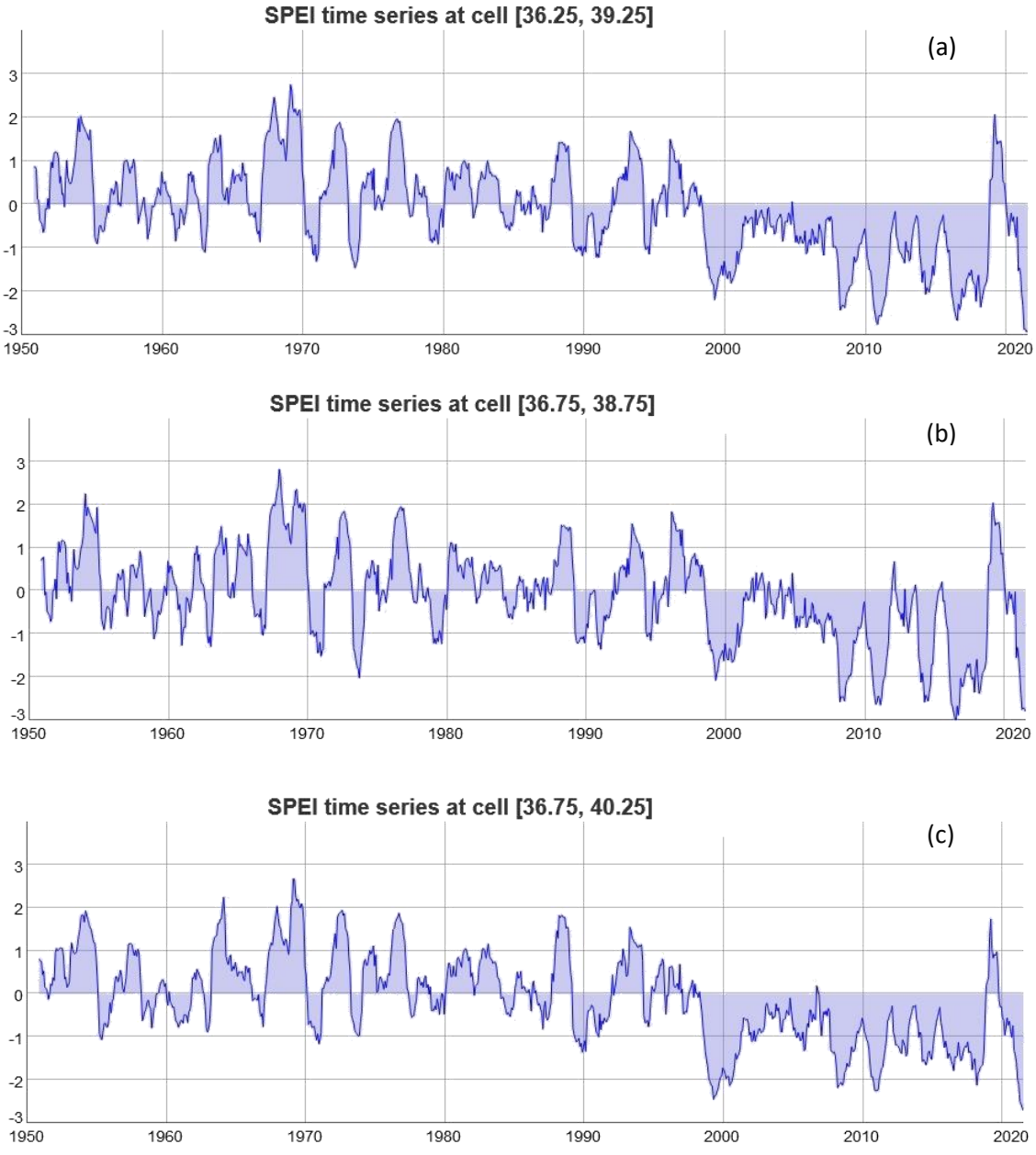

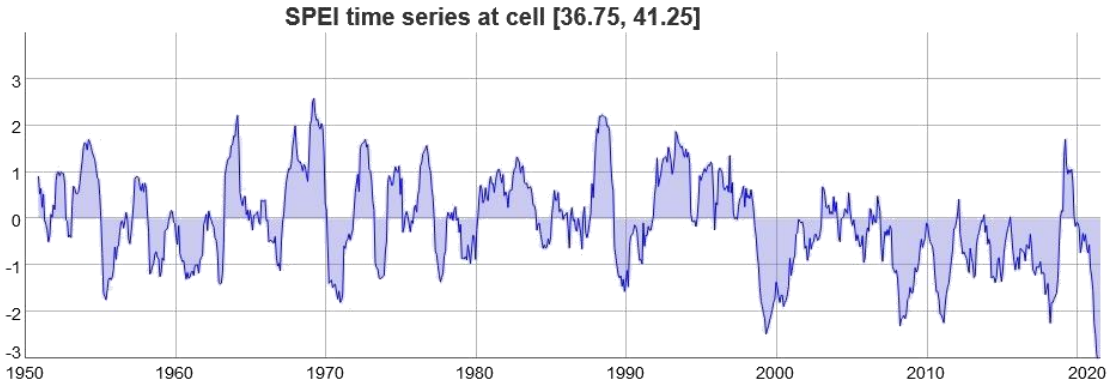


**Fig 22.** SPEI (Timescale: 12 months) changes of pixels in the study area between 1955 and 2021. The coordinates were given in the title of the graphs (Data source: SPEI, 2021).

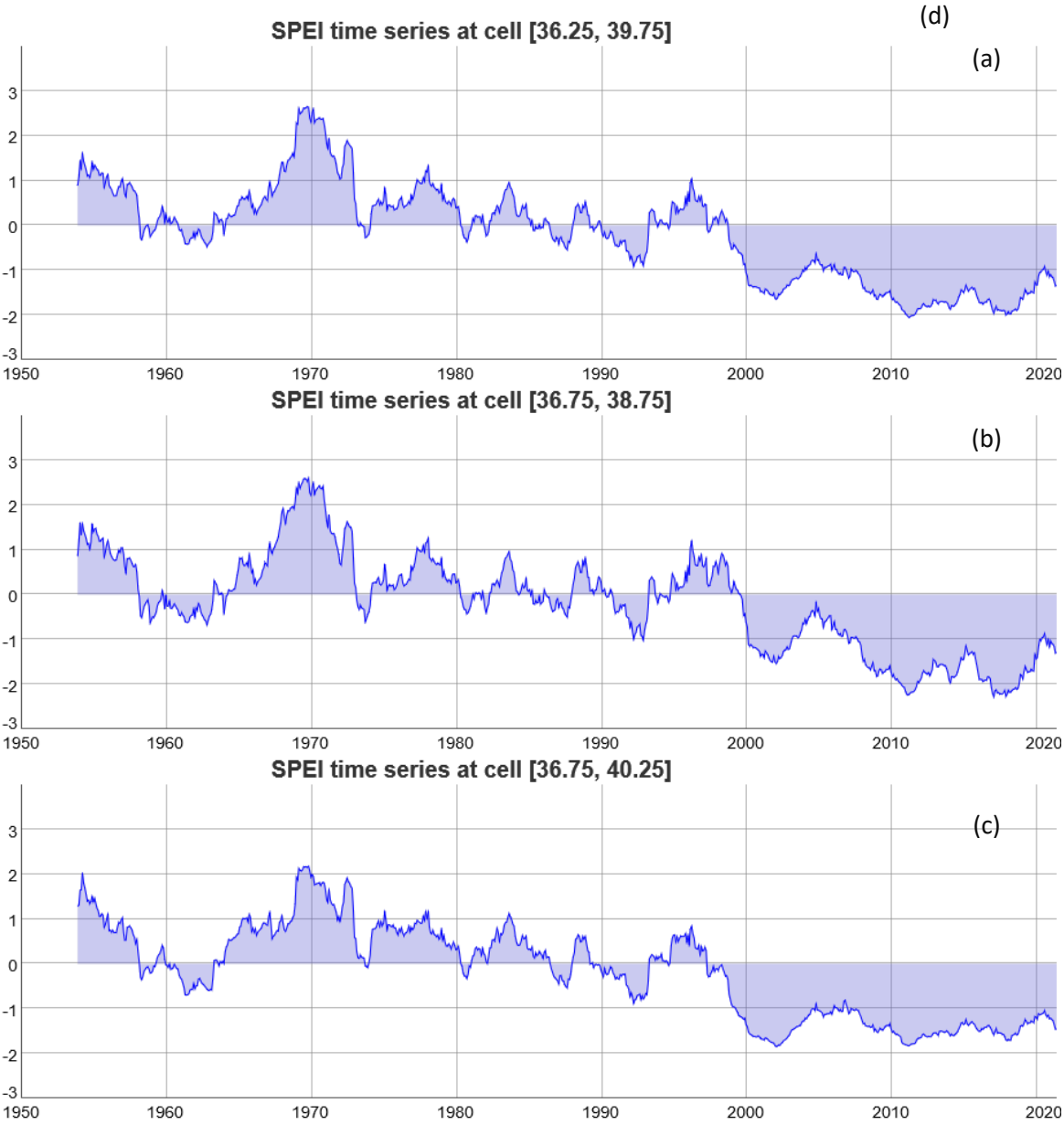

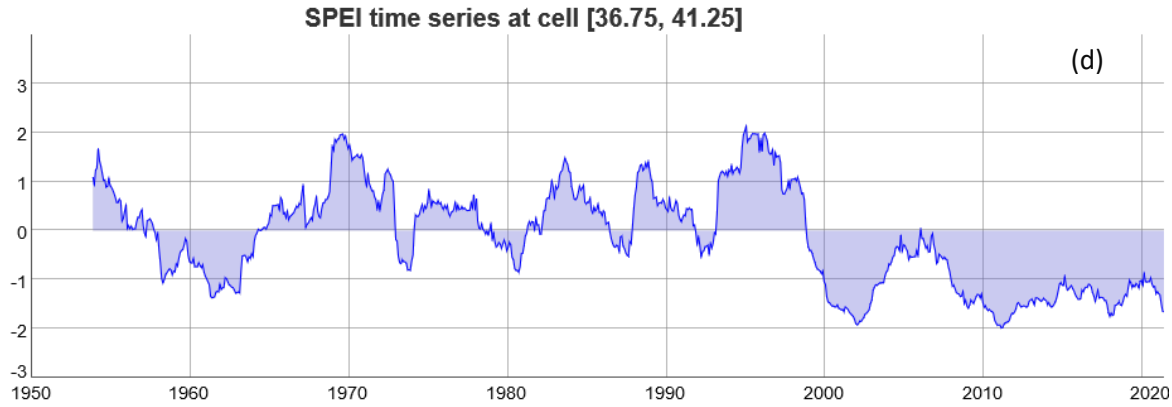


**Fig 23.** SPEI (Timescale: 48 months) changes of covered pixels between 1955 and 2021. The coordinates were given in the title of the graphs (Data source: SPEI, 2021).

Fig 22 (a) represents the west of the study area. These values remain within the borders of Syria. Although there are irregularities in precipitation between 1990-2000 in this region, there are positive SPEI values in this period. However, after 2000, a long dry period was experienced in the region until 2019. The long-term drought between 2000-2018 did not affect the groundwater values in the study area between 2003-2007 (Fig 18). Because, between 1990-2000, drought is not very severe, and precipitation is seen. Thus, groundwater was protected between 2003 and 2007. However, the decrease in precipitation and the increase in the transition to irrigated agriculture after 2000 (Fig 15) adversely affected groundwater, broadly preferred over time.

Figure 22 (b) represents the western part of the study area within the borders of Turkey. The dry period in this region again covers the period of 2000-2018. However, there was diminutive positivity in SPEI between 2002-2004. The drought between 2008-2010 is still severe. This condition also explains the low level of GWS in those years. The low precipitation in all pixels for the 2008-2010 period and the increase in groundwater use exacerbated the withdrawal. 2016 was the period when the most negative SPEI value between 2000-2020 was seen. In this region, it was determined that there was an increase in precipitation in 2019.

Fig 22 (c) represents the middle part of the study area. In this region, as in other pixels, it is seen that there is a long-term drought, except for 2019. For this reason, there is dense use of groundwater rather than surface water throughout the region. The high rate of drought and irrigated agriculture in this region has led to an irreversible decrease in groundwater (Fig 18).

Figure 22 (d) shows that the SPEI being positive in the northeastern part of the study area between 1991 and 1999 means that drought events did not intensify in the region. Sufficient precipitation did not affect the groundwater in this period and the following period between 2000-2007 (Fig 18). In fact, except for the dry period between 2000-2003, there was a relative increase in precipitation until 2006. After 2007, a long dry period was seen in this region until 2018. It is seen that SPEI was positive only in December of 2012. The year 2019 is the highest SPEI since 2000. The increase in the amount of precipitation also positively affected the groundwater.

According to the 48-month SPEI values analysed in Fig. 23, it is seen that a severe long-term drought has been experienced since 2000 (even if the intensity decreases in some years) throughout the study area, including all pixels.

### 4.5. Recent Drought, Agriculture, Water Management Stresses, and Links to Conflict

Over the past century (from 1900 to 2005), there were six major droughts in Syria. The average monthly level of winter precipitation—the primary rainfall season—dropped to around one-third of normal. Five of these droughts continued only one season: the sixth lasted two (Mohtadi, 2013).

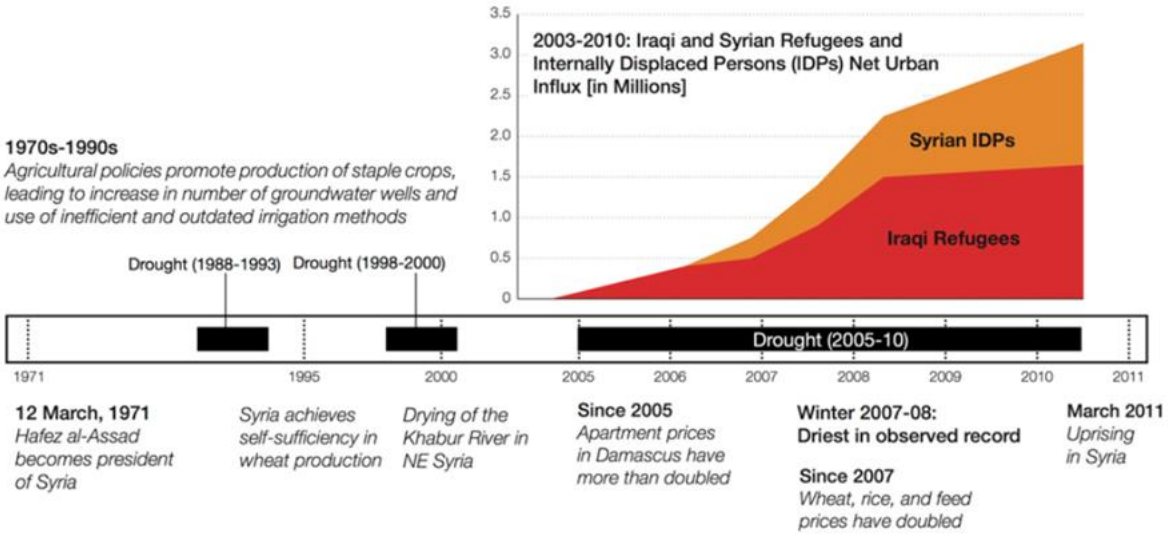


**Fig 24.** Timeline of events (Kelley and others, 2013).

Fig 24 shows how events in the region have evolved. (1) Drying of the Khabour river around 2000, (2) severe meteorological drought between 2005 and 2010, and (3) increase in the prices of crop plants that require water in this region are relatively compatible with land-use changes and temporal variations of the irrigation in agricultural lands (Fig 15).

According to data from 2005 (Fig 9, Fig 10, and Fig 11), northeastern Syria is a region where the irrigation of agricultural lands varies between 80% and 100%. In the study area, irrigation is generally employed with groundwater. As seen in the study, the use of groundwater, which has high availability (2003-2007), especially started to increase in the region in 2006 in the irrigated agricultural areas. Thus, the existence of the sufficient groundwater led to an increase in irrigated agricultural areas in this region until 2011 (Fig 15). This result is supported by Yılmaz and Peker (2013). However, the region experienced an intense drought from 2002 until 2018. As a result, Syria experienced a multiseason, multiyear period of extreme drought that contributed to agricultural failures, economic disruptions, and population displacement (Worth, 2010). This dry period has continued and is explained as the "worst long-term drought, and most severe set of crop failures since agricultural civilizations began in the Fertile Crescent many millennia ago" [Gary Nabhan, as cited by Femia and Werrell (2013)].

Drought also caused the groundwater to lose its ability to be fed by precipitation while being withdrawn by communities. Especially 2008 and 2009 (Fig 18) were the years when the groundwater decreased remarkably. As stated in Fig 24, this has led to an increase in the prices of water-demanding crops such as rice and feed. The sufficient precipitation in the region between 1970 and 1990 caused the decision-makers to irrigate agricultural lands with inefficient irrigation systems and drill too many wells in the region. However, the long-term drought in the region, especially after 2000, pushed the local people in the region to use groundwater more intensively, as can be seen in the 2005 data (Fig 9, Fig 10, and Fig 11). The inability to feed groundwater due to drought almost ended the expansion of the irrigated agricultural area in 2011, which had increased until 2011. 2011 was also the year that the uprising in Syria started.

In the current civil war, some specialists have argued that factors related to drought, including agricultural failure, water shortages, and water mismanagement, have played an essential role in contributing to the deterioration of social structures and spurring violence (FAO, 2012; Femia and Werrell 2013; Mhanna, 2013). In particular, the combination of severe drought, persistent multiyear crop failures, and related economic deterioration led to substantial dislocation and migration of rural communities to the cities. These factors further influenced the urban unemployment and economic dislocations, and social unrest.

## 5. CONCLUSIONS: CLIMATE CHANGE - AS A DRIVER OF FUTURE CONFLICTS IN THE REGION

Gleick (2014) argues that there is some evidence that the recent drought is an early indicator of the climatic changes that are expected for the region, including higher temperature, decreased basin rainfall and runoff, and increased water scarcity. Absent any efforts to address population growth rates, these water-related factors will likely produce even more significant local and regional political instability risks unless other mechanisms for reducing water insecurity can be identified and implemented.

In the region as a whole, decreasing water quality, growing water withdrawals, and limited political cooperation on water issues may become even more critical and lead to the securitization of water resources in coming years.

The pressure of climate change in Syria has contributed to mass migration, armed conflict, and ethnic division. Climate change model projections show that the current trend will continue and may lead to conflict between riparian states. Moreover, it can significantly change the basin-scale water equation and rise hydropolitics tension.

In the mid and long-term, drought and lower precipitation based on the climate models and projections represent a severe threat to the region's stability, as the competition for the limited resource will increase.

The future of water in the study area is threatening when the future projections were evaluated. While the current water stress in the study area is “low-medium” in the northeast, “extremely high” in the centre, and “high” in the west based on Aqueduct (2015), it will be “medium-high” in the northeast, “extremely high” in the centre and “high” in the west for all the scenarios, which are optimistic (SSP2 RCP4.5), business as usual (SSP2 RCP8.5) and

pessimistic (SSP3 RCP8.5), in 2030 and 2040. Water supply (total blue water (renewable surface water))[1] will be 10-30 cm in the entire study area for all scenarios.

The region is now, regrettably, more sensitive to the climate. In the past, the precipitation and sufficient groundwater caused the local people to shift their agricultural patterns to irrigated agriculture. However, human-induced excessive water withdrawal, increased drought, contaminated water, and climate change have caused this agricultural shift to be replaced by conflicts and uncertainties. Studies show that trends will continue, and the region requires a more collaborative, visioner, and mutually beneficial approach to take measures for these growing threats.

## References

ACAPS (2020). Syria Conflict Overview. Accessed at https://www.acaps.org/country/syria/crisis/conflict.

Albrecht, E., Schmidt, M., Mißler-Behr, M., & Spyra, S. P. (2014). Implementing Adaptation Strategies by Legal, Economic and Planning Instruments on Climate Change vol 4. Springer.

Amery, H. A. (2020). Malthus in the Middle East: Scarcity induced water conflicts. (Nile and Euphrates; Water and food as weapons). In book: Water and Conflict in the Middle East. Hurst & Company, London.

Aqueduct (2015). Aqueduct Water Stress Projections: Decadal Projections of Water Supply and Demand Using CMIP5 GCMs. In M. Luck, M. Landis, & F. Gassert (Eds). World Resources Institute.

AQUASTAT-FAO (2017). AQUASTAT - FAO's Global Information System on Water and Agriculture. http://www.fao.org/aquastat/en/geospatial-information/global-maps-irrigated-areas/map-quality. Accessed 24 September 2021.

Baba, A., Kareem R. A., & Yazdani, H. (2021). Groundwater resources and quality in Syria. Groundwater for Sustainable Development 14, 100617.

Begueria, S., Latorre, B., Reig, F., & Vicente-Serrano, S. M. (2021). Global SPEI database. https://spei.csic.es/database.html.

Copernicus Climate Change Service (2021). [Dataset]. Copernicus Climate Change Service's Land cover maps (2000 to 2020). https://cds.climate.copernicus.eu/cdsapp#!/dataset/satellite-land-cover?tab=doc.

ESA (2017). Climate Change Initiative - Land Cover led by UCLouvain.

Fanack.com (2019). Water Resources in Syria. https://water.fanack.com/syria/water-resources/.

FAO (2012). The Syrian Arab Republic Joint Rapid Food Security Needs Assessment (JRFSNA). FAO Rep., 26 pp. [Available online at http://www.fao.org/giews/english/otherpub/JRFSNA_Syrian2012.pdf.]

1 Projected change in total blue water is equal to the 21-year mean around the target year divided by the baseline period of 1950–2010 (Aqueduct, 2015).

FAO (2018). Special Report. In: FAO/WFP Crop and Food Security Assessment Mission to the Syrian Arab Republic, vol. 51p. Food and Agriculture Organization of The United Nations World Food Programme, Rome.

Femia, F., & Werrell, C. (2013). Syria: Climate change, drought, and social unrest. The Center for Climate and Security. [Available online at http://climateandsecurity.org/2012/02/29/syria-climate-change-drought-and-social-unrest/].

IFAD (2010). Syrian Arab Republic: Thematic study on land reclamation through defrocking. International Fund for Agricultural Development. Rome, Italy.

IHP-UNESCO (2017). [Dataset]. http://ihp-wins.unesco.org/maps/new.

GDO (2021). Analytical Report Global Drought Observatory: http://edo.jrc.ec.europa.eu/gdo 4 Drought in Syria and Iraq – April 2021 JRC Global Drought Observatory (GDO) of the Copernicus Emergency Management Service (CEMS).

Gleick, P.H. (2014). Water, drought, climate change, and conflict in Syria Weather. Climate, and Society, 6, 331-340.

Global Trade Analysis Project (GTAP) (2005). Global Agricultural Land Use Data for Integrated Assessment Modeling, in Human-Induced Climate Change: An Interdisciplinary Assessment. In: N. T. Ramankutty, H. Hertel, L. Lee, & S. K. Rose.

Graham, B., Muawia, B., Al-Maleh, A. K., & Sawaf, T. (2001). Tectonic and Geologic Evolution of Syria. GeoArabia, 6(4).

Kelley, C. P., Mohtadi, S., Cane, M. A., Seager, R., & Kushnir, Y. (2013). Climate Change and Political Instability in Syria. American Geophysical Union, Fall Meeting 2013, abstract id. GC13A-1047.

Lopez-Moreno, J. I., Vicente-Serrano, S. M., Zabalza, J., Begueria, S., Lorenzo-Lacruz, J., Azorin-Molina, C., & Moran-Tejeda, E. (2013). Hydrological response to climate variability at different time scales A study in the Ebro basin. Journal of Hydrology, 477, 175-188.

Mathbout, S., Lopez-Bustins, J. A., Martin-Vide, J., Bech, J., & Rodrigo, F. S. (2018). Spatial and temporal analysis of drought variability at several time scales in Syria during 1961– 2012. Atmospheric Research, 200, 153-168.

Mhanna, W. (2013). Syria's climate crisis. [Available online at http://www.al-monitor.com/pulse/politics/2013/12/syrian-drought-and-politics.html#].

Mohtadi, S. (2013). Climate change and the Syrian uprising. [Available online at http://thebulletin.org/web-edition/features/climate-change-and-the-syrian-uprising].

Mourad, K. A., & Berndtsson, R. (2012). Water status in the Syrian water basins. Open journal of modern hydrology, 2, 15, 01.

NASA Grace (2021). [Dataset]. Groundwater and Soil Moisture Conditions from GRACE-FO Data Assimilation for the Contiguous U.S. and Global Land. https://nasagrace.unl.edu/Default.aspx.

Salman, M., & Mualla, W. (2004). The utilization of water resources for agriculture in Syria: analysis of the current situation and future challenges. In: International Seminar on Nuclear War and Planetary Emergencies, pp. 263–274.

Siebert, S., Henrich, V., Frenken, K., & Burke, J. (2013). Global Map of Irrigation Areas version 5. Rheinische Friedrich-Wilhelms-University, Bonn, Germany / Food and Agriculture Organization of the United Nations. Rome, Italy: FAO.

Somi, G., Zein, A., Dawood, M., & Sayyed-Hassan, A., (2002). Progress Report on the Transformation to Modern Irrigation Methods until the End of 2001. Internal Report, MAAR (Ministry of Agriculture and Agrarian Reforms). Syria (in Arabic).

SPEI (2021). [Dataset]. SPEI Global Drought Monitor. https://spei.csic.es/map/maps.html.

UNOCHA (2019). Northeast Syria – As half a million people gradually regain access to safe water – the number of displaced people nears 180,000. Press release, 22 October 2019. Accessed at https://reliefweb.int/report/syrian-arab-republic/northeast-syria-half-millionpeople- gradually-regain-access-safe-water.

Ülker, D., Erguven, O., & Gazioglu, C. (2018). Socio-economic impacts in a Changing Climate: Case Study Syria. International Journal of Environment and Geoinformatics, 5(1), 84-93.

Varela-Ortega, C., & Sagardoy, J. A. (2002). Analysis of irrigation water policies in Syria: Current developments and future options. Proceedings of Irrigation Water Policies: Micro and Macro Considerations Conference, Agadir, Morocco, June.

Wada, Y., Beek, L., & Bierkens, M.F. (2012). Nonsustainable groundwater sustaining irrigation: a global assessment. Water Resources Research, 48 (6).

Worth, R. F. (2010). Earth is parched where Syrian farms thrived. New York Times, 13 October, New York ed., A1.

Zwijnenburg, W., Nahas, N., & Vasquez, R. J. (2021). War, Waste, and Polluted Pastures an Explorative Environmental Study of the Impact of the Conflict in north-east Syria. Development and Peace CARITAS CANADA.

Yılmaz, M. L., & Peker, H. S. (2013). A Possible Jeopardy of Water Resources in Terms of Turkey's Economic and Political Context: Water Conflicts [In Turkish]. Çankırı Karatekin Üniversitesi İktisadi ve İdari Bilimler Fakültesi Dergisi, 3(1), 57-74.

***Other Datasets:***

SPEI - https://soton.eead.csic.es/spei/index.html

NOAA NCEP CPC GHCN_CAMS - ftp://ftp.cpc.ncep.noaa.gov/wd51yf/GHCN_CAMS/

Global Precipitation Climatology Centre (GPCC) - ftp://ftp-anon.dwd.de/pub/data/gpcc/first_guess/

Article received: October 15 2021

Article accepted : November 17 2021